



UNIVERSITY POLITEHNICA OF BUCHAREST

Doctoral School of the Faculty of Applied Sciences



# **Communications Session for PhD students**

Session Program and Abstracts

**Bucharest**  
**25 May 2017**

## Session Program

25.05.2017

Room 2.2 - UPB Library

**OPENING SESSION****9:30-10:00**

- Welcome Address** *Prof. Horia IOVU, Director of CSUD*
- Opening Address** *Prof. Nicolae PUȘCAȘ, Director of Doctoral School*
- Keynote Address** *Eng. Drd. Bogdan Ștefăniță CĂLIN, Member of Doctoral School Board*

## PHYSICS

Room 2.2 - UPB Library

**SESSION ONE****10:00-12:00****Chair,** *Andreea Mitu, Doctoral School of the Faculty of Applied Sciences*

- 1. Implementing refraction correction for laser beam diagnostics and alignment at CETAL petawatt-class laser**  
*Mihail-Gabriel Bărbuță*
- 2. Polarization beam splitter design based on slab photonic crystals for two-photon polymerization direct laser writing**  
*Bogdan Ștefăniță Călin, Marian Zamfirescu, Radu Ionicioiu, Nicolae Puscas*
- 3. Investigation of dissimilar laser welding of stainless steel to aluminium in lap joints configuration**  
*G.D. Chioibașu, D. Klobčar, D. Sporea, S. Smolej and A. Nagode*
- 4. NO<sub>2</sub> total column amount from Pandora – 2S, comparison with satellite data: Preliminary results**  
*Alexandru Dandocsi, Anca Nemuc, Nicolae Puscas, Liliana Preda*
- 5. Laser matter interaction**  
*Ioana Dinicu (Spirea)*
- 6. A conservative or dissipative Universe? Gravitational viscosity and the space-time torsion. From COBE to Gravity Probe**  
*Cristian Gheorghiu*

**PAUSE****12:00-12:20**

**SESSION TWO****12:20-14:00****Chair, Mihail-Gabriel Bărbuță**, *Doctoral School of the Faculty of Applied Sciences***7. Thin film deposition using the pulsed laser method**Oana Andreea Lazăr**8. High grade decontamination of Ni targets for sub-barrier transfer reactions**Andreea Mitu, Marius Dumitru, Florian Dumitrache, Nicolae Marginean, Rareș Șuvailă,  
Cristina Niță, Maria Dinescu, Gheorghe Căta -Danil**9. The study of  $p$ -Si/TiO<sub>2</sub>/ $n$ -Si (100) sandwiches structures deposited by KrF excimer laser ablation**Călin Moise, Alin Jderu, Oana Brincoveanu, Dionizie Bojin, Marius Enăchescu**10. New digital acquisition system for alarge multichannel spectroscopy array**Lucian Stan**11. Assessment of a Hybrid Acquisition System for Positron Annihilation-based Spectroscopy**Sebastian Toma**CLOSING SESSION****14:00-14:20****Chair, Bogdan Ștefăniță CĂLIN**, *Doctoral School of the Faculty of Applied Sciences*

**MATHEMATICS**

Room 2.3 - UPB Library

**SESSION ONE****10:00-11:00****Chair,** *Ana-Maria BORDEI, Doctoral School of the Faculty of Applied Sciences***1. Implications of random processes theory by MS Excel and origin in the study of linear dynamic systems***Bogdan Cioruță, Nicolae Pop, Tudor Sireteanu***2. A functional equation of Butler-Rassias type and its Hyers-Ulam stability***Mihai Monea***3. Hydraulic servomechanism models with delay***Daniela Enciu, Andrei Halanay, Ioan Ursu***PAUSE****11:00-11:20****SESSION TWO****11:20-12:00****Chair,** *Daniela ENCIU, Doctoral School of the Faculty of Applied Sciences***4. Stochastic connectivity on almost-Riemannian structures induced by symmetric polynomials***Teodor Turcanu, Constantin Udriște***5. Stability analysis of some equilibrium points in a complex model for cells evolution in leukemia***Ana-Maria Bordei, Irina Badralexi, Andrei Halanay***CLOSING SESSION****12:00-12:20****Chair,** *Ana-Maria BORDEI, Doctoral School of the Faculty of Applied Sciences*

**Session PHYSICS**  
**abstracts**

# Implementing refraction correction for laser beam diagnostics and alignment at CETAL petawatt-class laser

Mihail-Gabriel Bărbuță  
Faculty of Applied Sciences, "Politehnica" University, Bucharest

## Abstract

Complex high-power laser installations which require multiple mirrors in high vacuum conditions also require multiple diagnostics points to ensure that the laser beam is properly aligned before starting experiments. In some cases, the diagnostics beam is acquired using transmitted (leaked) beam from the rear of the alignment mirrors, but the refractive index of these mirrors will induce a deviation of the diagnostics beam position, which itself varies according to the mirror relative inclination. Correcting this deviation needs to be implemented in automated and manual beam alignment systems, to avoid clipping and internal reflections which can be detrimental to laser system infrastructure.

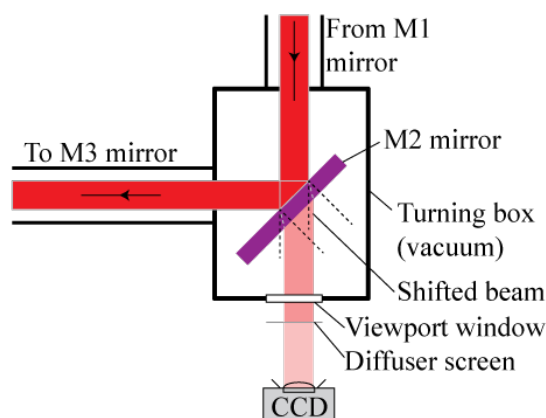


Fig. 1 – Conceptual representation of laser diagnostics beam displacement

For implementing refraction correction into beam alignment algorithms, an optical study has been conducted at INFLPR CETAL petawatt laser system, taking several factors into consideration: laser parameters, beam transport system design, mirror constructive details and material parameters. Beam deviation tests have been conducted at various mirror inclinations and results were compared with calculated deviation interval.

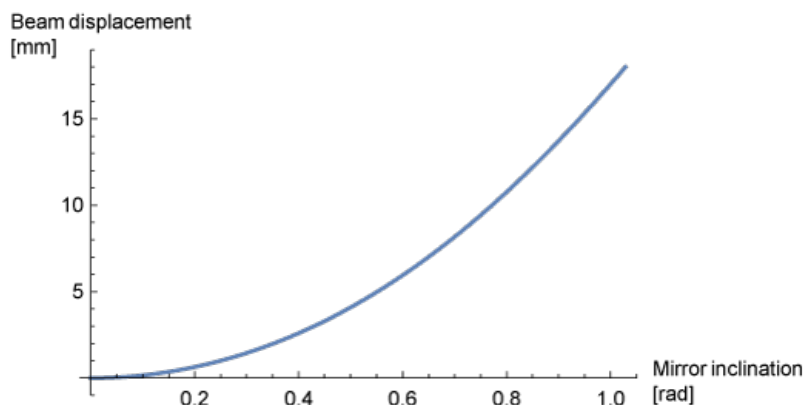
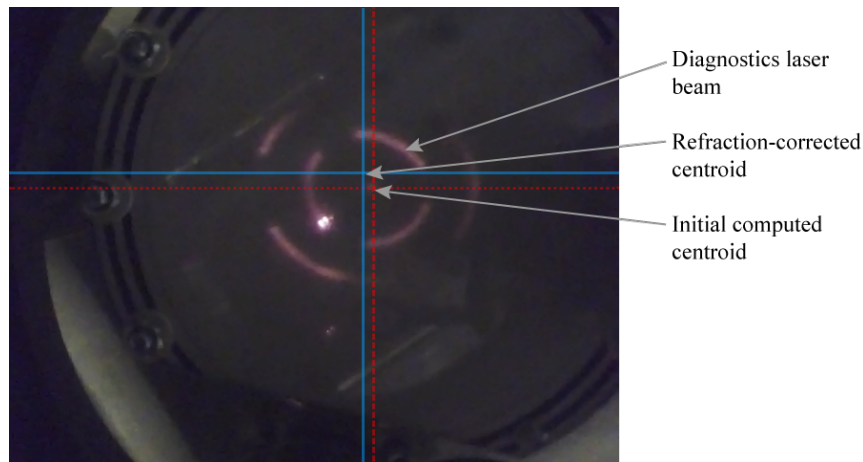


Fig. 2 – Calculated beam displacement variation function of mirror inclination (sapphire, 65 mm thickness, P-polarized laser beam)

The existing alignment algorithms for CETAL’s beam transport system were updated to include mirror-angle-driven refraction correction. Encoded mirror inclination values are captured, and corresponding refraction deviation is automatically calculated by an additional algorithm written in Python programming language. The alignment software then calculates the correct beam centroid. This implementation resulted in significant improvement in alignment and beam centering accuracy, correcting centering calculations for diagnostics beam shifts up to 18 mm in extreme mirror tilt situations.



*Fig 3 – Laser beam centering diagnostics with initial and corrected centroid calculation*

Scientific literature search has revealed no previous studies of refraction correction for laser beam diagnostics and alignment. This solution can be implemented in existing and future high-power laser systems to aid in achieving higher alignment precision and efficiency, and can be easily adapted to various material and laser parameters.

**List of references:**

1. Wolf, K. B., “Geometry and dynamics in refracting systems”, European Journal of Physics 16: 14-20, 1995
2. ARDoP SAS, “CETAL Project – Beam Line Transportation – Final design”, 2013
3. Harman, Alang Kasim; Ninomiya, Susumu; Adachi, Sadao, "Optical constants of sapphire (alpha-Al<sub>2</sub>O<sub>3</sub>) single crystals". Journal of Applied Physics. 76 (12): 8032–8036 (1994)

# POLARIZATION BEAM SPLITTER DESIGN BASED ON SLAB PHOTONIC CRYSTALS FOR TWO-PHOTON POLYMERIZATION DIRECT LASER WRITING

B. Calin<sup>1</sup>, M. Zamfirescu<sup>1</sup>, R. Ionicioiu<sup>2</sup>, N. Puscas<sup>3</sup>

Integrated polarization beam splitters and photonic crystals represent complex optical microstructures with various applications. Photonic crystals may be used in fiber fabrication for more efficient light confinement [1] or as wavelength filters [2], due to the existence of photonic band gaps. Furthermore, these band gaps can manifest for specific polarizations of incident light, which not only extends the applications of photonic crystals as filters, but they can also be employed in complex optical structures that act as polarization beam splitters [3], [4], [5].

In this paper, a complex photonic structure acting as a narrow-band polarization beam splitter is discussed. Apart from a two-dimensional photonic crystal with a TE band gap centered around a wavelength of 780 nm, the device is comprised of linear waveguides, parabolic light “collectors” (parabolic tapered waveguides) and multimode interference couplers. A schematic of the device is presented in figure 1.

A step-by-step methodology for the optimization of the photonic crystal is presented. Device fabrication is also addressed as the targeted method is based on two-photon polymerization direct laser writing. Experimental results are discussed and compared to other largely utilized methods such as simple direct laser writing [6], lithography [7], autocloning [8] and others [2].

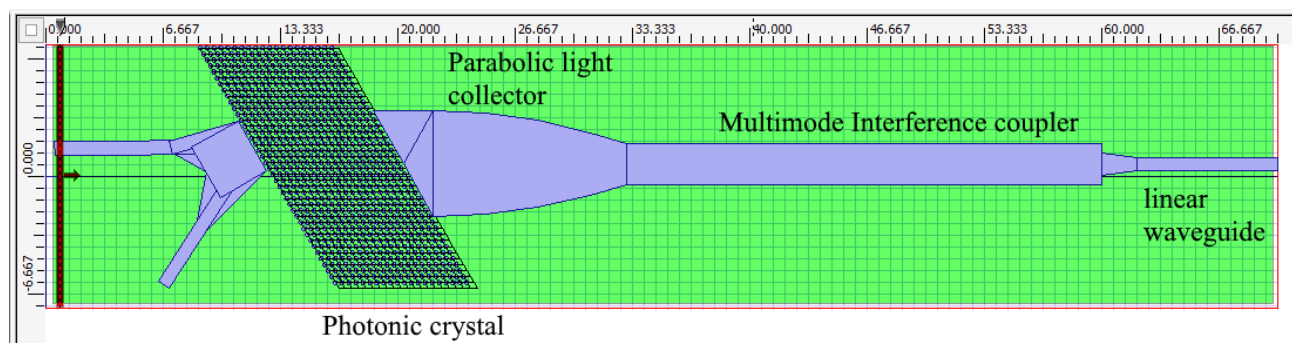


Figure 1: Polarization beam splitter design.

## REFERENCES

- [1] J. Kim, H. K. Kim et. al., The Fabrication of a Photonic Crystal Fiber and Measurement of its Properties, Journal of the Optical Society of Korea, **vol. 7**, no. 2, pp. 79-83, (2003);
- [2] Y. Ohtera et. al., Ge/SiO<sub>2</sub> Photonic Crystal Multichannel Wavelength Filters for Short Wave Infrared Wavelengths, Japanese Journal of Applied Physics, **vol. 46**, no. 4A, pp. 1511-1515, (2007);
- [3] E. Schonbrun et. al., Polarization beam splitter based on a photonic crystal heterostructure, Optics Letters, **vol. 31**, no. 21, pp. 3104-3106, (2006);
- [4] J. She et. al., High-efficiency polarization beam splitters based on a two-dimensional polymer photonic crystal, Journal of Optics A: Pure and Applied Optics, **vol. 8**, pp. 345-349, (2006);
- [5] W. Zheng et. al., Integration of a photonic crystal polarization beam splitter and waveguide bend, Optics Express, **vol. 17**, no. 10, pp. 8657-8668, (2009);
- [6] J. Haberko et. al., Fabrication of mesoscale polymeric templates for three-dimensional disordered photonic materials, Optics Express, **vol. 21**, no. 1, pp. 1057-1065, (2013);
- [7] M. Belotti et. al., All-optical switching in 2D silicon photonic crystals with low loss waveguides and optical cavities, Optics Express, **vol. 16**, no. 15, pp. 11624-11636, (2008);
- [8] C. C. Cheng et. al., New fabrication techniques for high quality photonic crystals, Journal of Vacuum Science and Technology B, **vol. 15**, no. 6, pp. 2764-2767, (1997);

# Investigation of dissimilar laser welding of stainless steel to aluminium in lap joints configuration

G.D. Chioibaşu<sup>1</sup>, D. Klobčar<sup>2</sup>, D. Sporea<sup>1</sup>, S. Smolej<sup>3</sup> and A. Nagode<sup>3</sup>

1. National Institute for Laser Plasma and Radiation Physics, 077125 Magurele, Romania

2. University of Ljubljana, Faculty of Mechanical Engineering, Aškerčeva 6, 1000 Ljubljana, Slovenia

3. University of Ljubljana, Faculty of Natural Sciences and Engineering, Aškerčeva 12, 1000 Ljubljana, Slovenia

*Due to the many advantages given by dissimilar materials welded joints, like weight saving, reduction of pollutant emissions, the application of different welding components made of steel and aluminium alloys is still researchable. Laser fiber welding in a lap joint configuration of low carbon stainless steel, SS 316 L and A1050 aluminium alloy with 1 mm thick is presented. Tests that have undergone procedures are: tensile tests, optical metallography and scanning electron microscopy. A fibre laser with 400 W power in CW mode was used and the process parameters like speed and focusing position were optimized.*

**Keywords:** Dissimilar SS - Al welding; Fiber Laser welding; Lap joint configuration; Tensile strength.

## 1. Introduction

Welding dissimilar materials technology is continuously growing, but is a big challenge in engineering, because of the many advantages that this process offers to industry. Such as, good mechanical properties and corrosion resistance [1]. Joining stainless steel and aluminium reduce the weight of the car body and the consumption of fuel [2]. In laser welding the process parameters, like laser power, welding speed and focused position are essential. The optimized values of this factors can be obtain by using numerical optimization [3].

## 2. Experimental procedures

In the present study, the materials used were a low carbon stainless steel, SS 316 L and A1050 aluminium alloy with 120 mm x 40 mm x 1 mm. The chemical composition and mechanical properties are presented in the Table 1 and 2, respectively. Both materials were cleaned with alcohol and dried at warm air before welding, in order to get best quality of welds.

Table 1 Chemical composition of AISI 316L and A 1050(weight %).

Material	Elements (wt %)									
	C	Si	Mn	P	S	Cr	Mo	Ni	N	Fe
AISI 316 L	≤0.03	≤0.7	≤2	≤0.04	≤0.03	18	2-3	10-14	≤0.1	Balance

Material	Elements (wt %)							
	Cu	Mg	Si	Fe	Mn	Zn	Ti	Al
A 1050	≤0.05	≤0.05	≤0.25	≤0.4	≤0.05	≤0.07	≤0.05	Balance

A fiber laser was used for welding experiments, with a maximum power of 400 W in continuous mode (IPG Photonics, model YLR-400-AC, wavelength 1070 nm). A three-dimensional scanning head (HighYAG, RLSK) was attached to a six axis robot machinery (Motoman MC2000). During the welding process a cooper backing plate was under the working pieces to absorb a part of the head due to the laser processing.

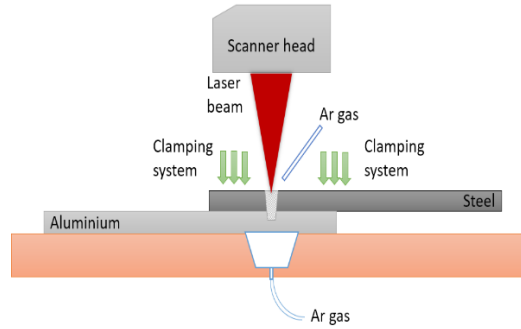
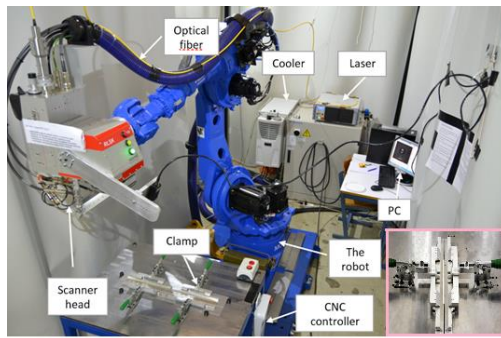


Fig. 1. Set-up experiment

### 3. Results and analysis

Five sets of optimized welding parameters process were performed in order to confirm the valability of the optimal results. SEM analysis (fig. 2) and macro-section of optimized weld were carried out to verify the quality of the welds.

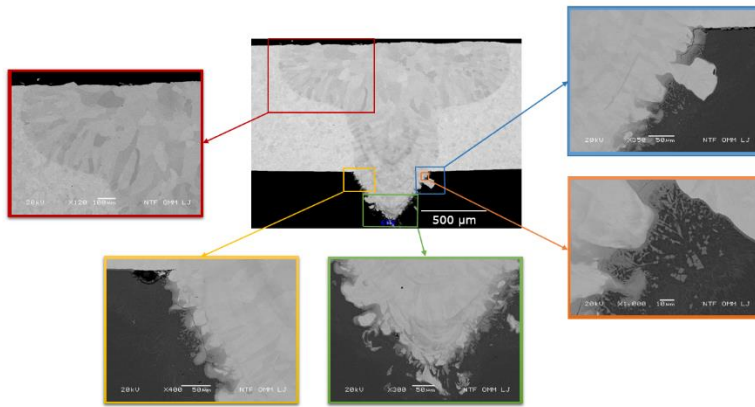


Fig. 2 SEM analysis of optimized weld

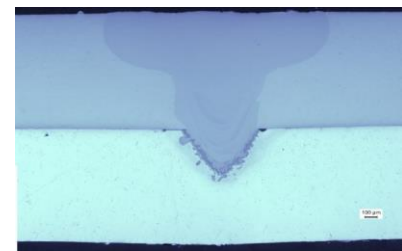


Fig. 3 Macro-section of optimized weld

### 4. Conclusions

- ✓ The best value of tensile strength it was achieved when a small part of stainless steel was meld into aluminium
- ✓ As deeper the weld is so many crack and defects appear
- ✓ The best weld was obtained by using 1.5 m/min speed and 0.5 mm defocus

### References

1. Chen, S., Huang, J., Xia, J., Zhao, X., & Lin, S. *Influence of processing parameters on the characteristics of stainless steel / copper laser welding*, Journal of Materials Processing Technology. 222, 43–51, (2015).
2. Sierra G, Wattrisse B, Bordreuil C. *Structural analysis of steel to aluminium welded overlap joint by digital image correlation*. Exp Mech (2008).
3. A. Ruggiero , L.Tricarico , A.G.Olabi , K.Y.Benyounis, *Weld-bead profile and costs optimisation of the CO2 dissimilar laser welding process of low carbon steel and austenitic steel AISI 316*, Optics & Laser Technology, 43 ,82–90 (2011)

# **NO<sub>2</sub> total column amount from Pandora – 2S, comparison with satellite data: Preliminary results**

A. Dandocsi<sup>1,2</sup>, A. Nemuc<sup>1</sup>, N. Puscas<sup>2</sup>, L. Preda<sup>2</sup>

<sup>1</sup>National Institute of R&D for Optoelectronics, Magurele, Romania, \*e-mail: [alexandru.dandocsi@inoe.ro](mailto:alexandru.dandocsi@inoe.ro)

<sup>2</sup>University Politehnica of Bucharest, Romania

## **Introduction**

The NO<sub>2</sub> is an important atmospheric pollutant that can be toxic in certain concentrations and the chemical reaction within the atmosphere (NO<sub>x</sub> = NO + NO<sub>2</sub>) leads to the production of ozone and aerosols. It is mainly produced by the anthropogenic activities like industry, traffic, forest fires but it can be produced in the natural way also [1].

The NO<sub>2</sub> total column amount is monitored from the satellite instruments since 1995, last system launched with this purpose being Ozone Monitoring Instrument (OMI), launched in 2004. Ground based measurements from a Pandora – 2S system, part of the Pandonia network ([www.pandonia.net](http://www.pandonia.net)) are used in comparison with OMI retrieval in order to participate in the calibration / validation activities of the satellite. Other similar studies have been made by [2]

## **Instruments description**

The Pandora – 2S system is a Multi Axis Differential Optical Absorption Spectroscopy system capable of having direct Sun/Moon measurements or measurements at different zenith and azimuth angles. The system has two spectrometers, ranging from 290 nm to 900 nm with a 0.6 nm resolution for the first spectrometer and a 1.1 nm resolution for the second spectrometer. The system uses direct Sun/Moon measurements in order to retrieve the total column amount of NO<sub>2</sub> and O<sub>3</sub>. The AirMassFactor (AMF), factor needed for the total column amount calculation, is obtained using the secant of the Solar Zenith Angle (SZA). For SZA greater than 80°, spherical atmosphere corrections must be applied [2]. Global measurements of NO<sub>2</sub> are made using the Ozone Monitoring Instrument placed on board of the Dutch-Finnish satellite of NASA, Aura EOS (Earth Observation System). The measurements are provided almost daily with a nominal spatial resolution of 13 x 24 km<sup>2</sup> at nadir since October 2004[3]. The NO<sub>2</sub>, among other trace retrieval is made using the solar backscatter light in the UV-VIS spectral range, measured by a two-dimensional CCD (charge-coupled device) detector.

The total column amounts of NO<sub>2</sub> from both systems were retrieved using the fixed location of the Pandora system which is near Bucharest, at approximately 12 kilometers from the city center, in the southern region. The pre-urban area, where the Pandora is located, is influenced from the highly active ring road traffic but also from the rural area, agricultural activities. In other words, the location is equally influenced by both natural and anthropogenic emissions.

## **Methodology**

Retrieval of total column amount of NO<sub>2</sub> is based on direct sun measurements and it can be done using both spectrometers, using the absorption cross section from [4]. The satellite data are retrieved using the solar backscattered light in the UV-VIS region but the NO<sub>2</sub> total column amount is calculated using the similar processing as for the ground based measurements.

For this paper, the level 2 global gridded data were used with a 0.25 deg. x 0.25 deg. resolution. Each data point selected for this study was carefully investigated. The location was selected within a ± 0.4 deg. from the ground based system. After that, the cloud cover parameter was taken into consideration so the data should not be influenced by the high reflectivity of the clouds.

From the ground based measurements point of view, data were selected around the time of the satellite overpass with a  $\pm 1$  hour bias, and then the mean value and its error were computed. Another way of using satellite data is to take only the automatically generated measurements for different locations(gome). This data file contains only the latitude and longitude of the measurement and the total column amount of interested absorber. The spectral range from which the total column of NO<sub>2</sub> is computed is between 400 nm and 440 nm for the Pandora system and 405 nm and 465 nm for the satellite data.

## Results and discussions

Two months of ground based measurements of total column amount of NO<sub>2</sub> was selected for this study. For comparison Starting from the satellite data described in the methodology section and then selecting the Pandora measurements, the total column amount of NO<sub>2</sub> was computed.

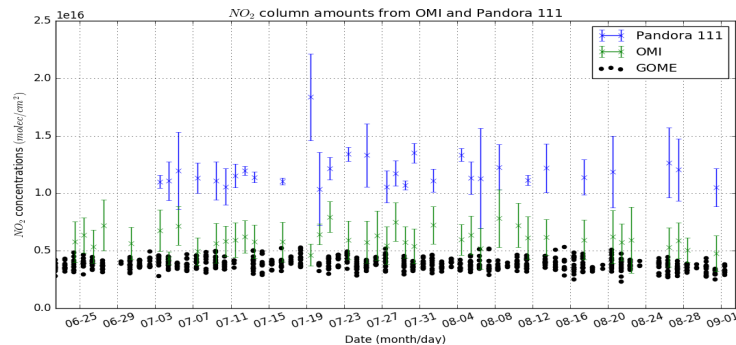


Figure 1 Total column amount of NO<sub>2</sub> from Pandora measurements and OMI satellite, July – August 2016

Figure 1 shows retrievals from ground based and satellite instruments where the black marker was used for the automatically generated data from satellite measurements around a fixed location. The difference between the two systems could be explained by different calibration procedures of each of the instruments. The Pandora system it is calibrated using a 9 step process using clear sky measurements as described by [2]. Data selected from the level 2 gridded measurements show similar trend to the ones from Pandora as they tend to have similar variation from day to day while the automatically generated data tend to be more stable (Not Shown).

## Conclusions

Total column amount of NO<sub>2</sub> from a ground based instruments was retrieved in order to be compared with coincident satellite measurements and a period of two months is presented here. One algorithm of data selection from satellite measurements is presented in order to compare the total column amounts of NO<sub>2</sub> with the ground based measurements. A bias in the absolute values from the two instruments, further analysis will be done.

## References

- [1] Wenig, M. O., et.al. (2008), Validation of OMI tropospheric NO<sub>2</sub> column densities using direct-Sun mode Brewer measurements at NASA Goddard Space Flight Center, *J. Geophys. Res.*, **113**, D16S45, doi:10.1029/2007JD008988
- [2] J. Herman, et.al., NO<sub>2</sub> column amounts from ground-based Pandora and MFDOAS spectrometers using direct-sun DOAS technique: Intercomparison and application to OMI validation, *Journal of Geophysical Research*, Vol. 114, D13307, doi:10.1029/2009JD011848, 2009
- [3] Levelt, P. F., et. al.: *The Ozone Monitoring Instrument*, *IEEE T. Geosci. Remote*, **44**, 1093–1101, doi:10.1109/TGRS.2006.872333, 2006.
- [4] Vandaele, A.C., et.al., Measurements of the NO<sub>2</sub> absorption cross-section from 42 000 cm<sup>-1</sup> to 10 000 cm<sup>-1</sup> (238-1000 nm) at 220 K and 294 K, *J. Quant. Spectrosc. Radiat. Transfer*, **59** (3-5), 171-184, 1998

# LASER MATTER INTERACTION

AUTHOR: Dinicu (Spirea) Ioana

GUIDING TEACHER: Prof. Univ. Dr. Nicolae PUȘCAȘ

## Summary

In this paper, the fundamental theoretical and numerical approaches developed to analyse laser–target interaction, plasma formation, as well as its expansion will also be reviewed, and their predictions compared with the experimental findings. Although the main emphasis of the review will be on metal target ablation, reference and comparison to results on multicomponent targets will also be frequently given. The generation of high-density and high-temperature plasmas by focusing high peak power laser radiation onto a solid target is still a growing field in basic science, engineering and material processing technology (Von Allmen and Blatter 1995, Miller and Haglund 1998), though the interaction of laser light with materials and the properties of the plasma produced have been investigated for many years (Kennedy 1984). The strong interest in this field is largely due to the fact that both fundamental aspects of laser–solid interaction and consequent plasma generation, and applied techniques in material processing technology and sample elemental analysis are involved (Bauerle 1984, 1996).

Since laser ablation depends on the target thermo-physical properties and laser beam parameters. The scope of the paper is to study, especially, the ablation process of simple one-component materials such as metals (**ex. Al, Cu, Fe**) which allow a better comprehension of the basic mechanisms involved in laser–solid and laser–plasma interaction. Since the thermo-physical properties of metals are comparatively well known, they will be compared to experimental data.

Is taken into account the *adiabatic limiting case* description of the process: the decoupling of these processes (heating and expansion of the ablated material).

The interaction of high-intensity laser pulses with a solid target involves laser–solid interaction and plasma formation. The process can be divided into two different regimes:

1. at low laser fluence the vapour produced by the leading edge of the laser pulse behaves like a thin medium and the laser beam passes nearly unattenuated through the vapour.
2. at high laser fluence the vapour temperature is high enough to cause appreciable atomic excitation and ionization. Then the vapour begins to absorb the incident laser radiation leading to vapour breakdown and plasma formation.

Laser systems with pulse durations variable from about 100 fs to several nanoseconds allow to perform a very detailed analysis of the laser–matter interaction at different laser pulse durations, leaving the other laser parameters almost unchanged.

In order to understand the basic characteristics of the laser–solid interaction, simple approximated calculations based on energy balance considerations can be applied. This allows an estimation of the order of magnitude of the laser fluence threshold for vaporization, the amount of material evaporated per pulse, as well as its dependence on the laser fluence.

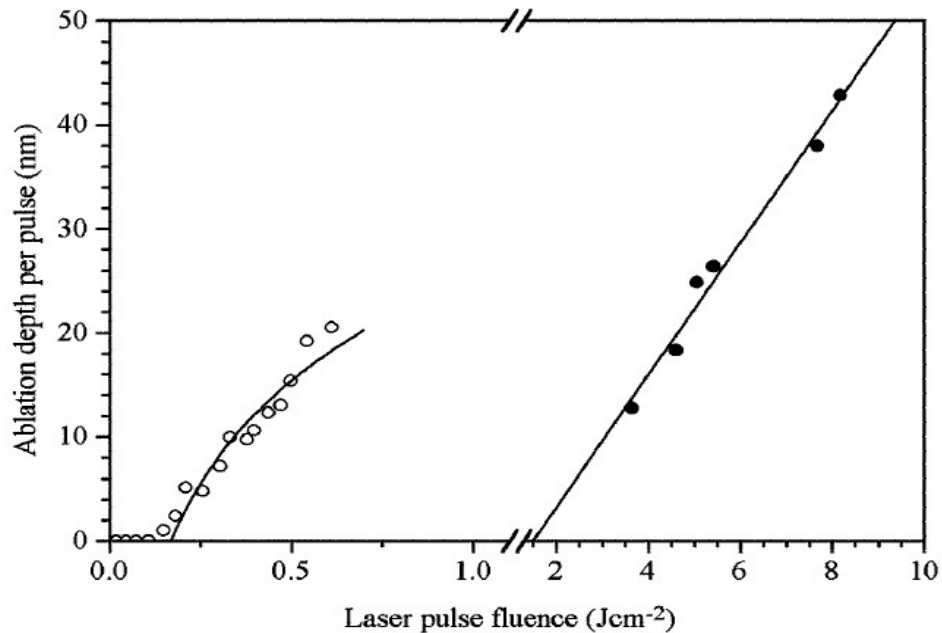
Both the basic physics of the laser–solid interaction and the experimental results show that short laser pulses (610 ps FWHM) offer the advantage of removing material from the target surface without a significant transfer of energy to the surrounding areas, what is of interest in the field of micro-machining and in material processing applications.

Table 1:

Theoretical and experimental fluence threshold, penetration length (short pulse) and absorbance (long pulse) for copper laser ablation at 248 nm. The discrepancy between the absorbance standard-reference book value and the experimental one can be ascribed to the target shielding due to the vapour formed above the target surface.

Pulse duration = 0.5 ps		Pulse duration = 20 ns	
$F_{th}$ (J cm <sup>-2</sup> ) calculated	0.10	$F_{th}$ (J cm <sup>-2</sup> ) calculated	1.2
$F_{th}$ (J cm <sup>-2</sup> ) fit to equation (5)	0.17	$F_{th}$ (J cm <sup>-2</sup> ) fit to equation (5)	1.5
$\alpha^{-1}$ (nm) literature	14	A literature	0.6
$\alpha^{-1}$ (nm) fit to equation (5)	14.3	A fit to equation (7)	0.03

**Figure 1.** Ablation depth per pulse versus fluence for 248 nm KrF laser ablation of copper in vacuum: ○, short pulse (0.5 ps) (after Preuss *et al* 1995); ●, long pulse (20 ns) (after Lunney 1995). The full curves are fits according to equations (4) and (6), respectively.



## References

- Amoruso S 1998 *PhD Thesis* Universit`a degli Studi di Napoli 'Federico II', Naples  
 —1999 *Appl. Surf. Sci.* **138–139** 292  
 Amoruso S, Armenante M, Berardi V, Bruzzese R and Spinelli N 1997 *Appl. Phys. A* **65** 265  
 Amoruso S, Berardi V, Bruzzese R, Spinelli N and Wang X 1998 *Appl. Surf. Sci.* **127–129** 953  
 Amoruso S, Berardi V, Bruzzese R, Velotta R and Armenante M 1996 *Appl. Phys. A* **62** 533  
 Amoruso S, Bruzzese R, Velotta R, Spinelli N and Wang X 1999 *Appl. Surf. Sci.* **138–139** 250  
 Afonso C N, Serna R, Catalina F and Bermejo D 1990 *Appl. Surf. Sci.* **46** 249  
 Alimpiev S S, Belov M E, Mlinsky V V, Nikiforov S M and Romanjuk V I 1994 *Appl. Phys. A* **58** 67  
 Bauerle D (ed) 1984 *Laser Processing and Diagnostics* (Berlin: Springer)  
 —1996 *Laser Processing and Chemistry* (Berlin: Springer)  
 Bekefi G, Deutsch C and Yaakobi B 1976 *Principles of Laser Plasmas* ed G Bekefi (New York: Wiley) pp 549–641  
 Berardi V, Amoruso S, Spinelli N, Velotta R, Allegrini M and Arimondo E 1994 *J. Appl. Phys.* **76** 8077  
 Berardi V, Amoruso S, Spinelli N, Velotta R, Fuso F and Arimondo E 1995 *Int. J. Mass Spectrom. Ion Phys.* **144** 1  
 Berardi V, Spinelli N, Velotta R, Armenante A, Fuso F, Allegrini M and Arimondo E 1993 *Phys. Lett. A* **179** 116  
 Boardman A D, Cresswell B and Anderson J 1996 *Appl. Surf. Sci.* **96–98** 55  
 Callies G, Schittenhelm H, Berger P and Hugel H 1998 *Appl. Surf. Sci.* **127–129** 134  
 Carslow H S and Jaeger J C 1959 *Conduction of Heat in Solids* (Oxford: Oxford University Press)  
 Caruso A and Gratton R 1968 *Plasma Phys.* **10** 867

Presentation of work: oral presentation (Microsoft Power Point)

Date: 5 April 2017

# **A conservative or dissipative Universe? Gravitational viscosity and the space-time torsion. From COBE to Gravity Probe**

Cristian Gheorghiu<sup>1</sup>

The aim of this paper is to answer the question: "Why are most phenomena in the Universe irreversible" when the theoretical physics is based mainly on conservative principles: energy, impulse or angular momentum!? We know from the 2<sup>nd</sup> principle of thermodynamics that the general entropy of the Universe only increases and the Universe is deeply dissipative. Paradoxically, physics is generally oriented on the study of the so called " body- forces " : gravitation, electromagnetism, inertial forces, etc. which are conservative fields . But opposed to the body-forces are the so called contact-forces (meaning friction forces, normal forces or viscous forces) which are dissipative and consequently are responsible for the irreversibility of the phenomena of the Universe. In this paper we analyze the primary source of the existence of these dissipative contact forces , namely the space-time's viscosity (i.e. gravitational viscosity [1] ). Andrei Linde said that "...scalar field equations that describe the Quantum Vacuum are susceptible to the term of a viscosity ..." [2] . Therefore, we assume the Universal space-time itself as being a viscous fluid and not a perfect one as considered in the General Theory of Relativity (GRT). The main argument for such a hypothesis is the anisotropy measured by COBE in the CMB (Cosmic Microwave Background) in 1993 [3] . In order to test the validity of the value obtained in the paper for the space-time viscosity, we calculate within the paper the space-time's torsion around the Earth (already anticipated by the GRT and confirmed experimentally by the Gravity Probe in 2004 ): hence the novelty of this study is given by the interpretation of the space-time as a viscous fluid, and the gravitational torsion as a vortex appearing as a Oseen type solution for the Navier-Stokes equation applied to the movement of the Earth through it..

The main result of this article is the determination of the viscosity of the space-time  $\eta_0$  (named - gravitational viscosity ) using 2 different methods (chapter 2) respectively the method of autocorrelation functions from the Kubo-Green formula, applied to the anisotropies measured by COBE (fig 1 ) but also the method of the kinetic-molecular theory for gases. In chapter 4 we have used the value for the gravitational viscosity to calculate the space-time torsion ( fig 2 ) in conditions similar to the experiment Gravity Probe B and the value obtained here is similar to the frame dragging-drift rate(anticipated by Einstein in GRT ) and measured by the Gravity Probe B. This result encourages the use of the viscous fluid model for the space-time in other astrophysics theories. In chapter 5 we have determined, using the Stokes method, the energy lost by the Earth by viscous friction with the space-time in its relative movement through the CMB with the speed of 390 km/s (also determined by COBE). In the end, we have proposed an improved calculation formula for the damping of the Gravitational Waves through the Vacuum . Another major effect of the viscous model of the space-time is that the relative speed Earth - CMB must be reduced incrementally with the acceleration . This BRAKING phenomenon of the Earth compared with the CMB, requires the existence of an Inertial Mass independent of the presence of other bodies ! This would fundamentally contradict Mach's principle . In our opinion, the energy losses by gravitational viscosity[1]

represent a major cause of the irreversibility of the phenomena at a cosmological scale.

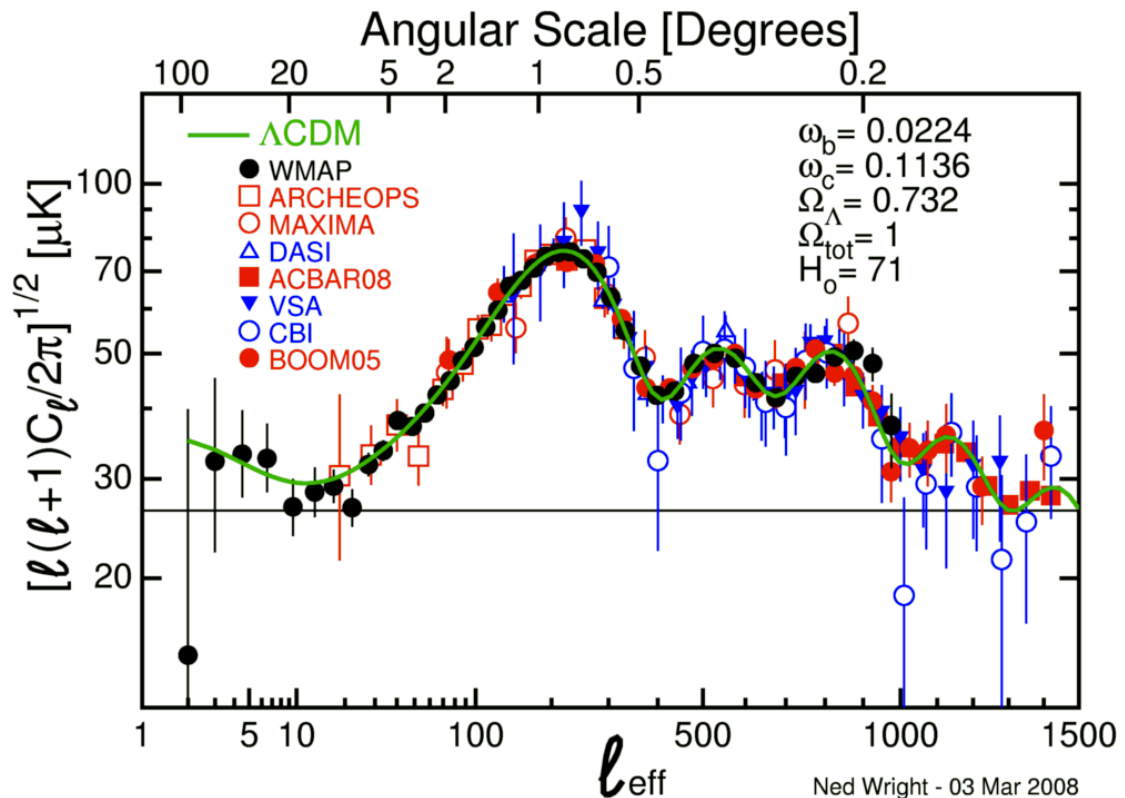


**fig 1** - CMB thermal variations -anisotropies (function to solid angle) measured by COBE , WMAP , Boomerang & all.[3].

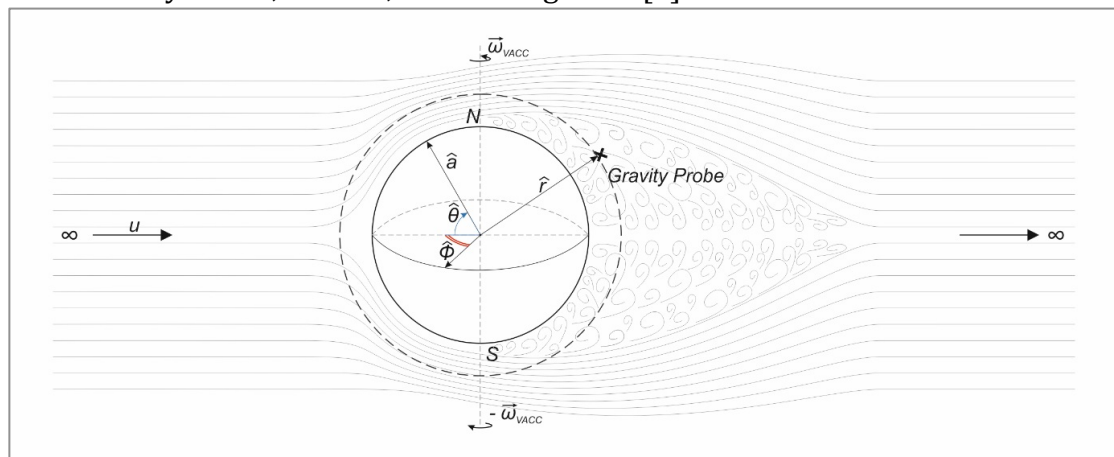


**fig 2**- Earth moving with  $u$ -speed trough viscous space-time ;  $(\hat{r}, \hat{\theta}, \hat{\phi}) =$  spherical coordinates ;  $\omega_{vacc}$ = space-time vorticity ( torsion ) to the North Pole and to the South Pole ;  $a$ = Earth radius .

[1] *E Fischer*- Energy loss by gravitational viscosity -General relativity and quantum cosmology mai 2008 / pg 1-7

[2] *A Linde* - L'inflation eternelles de l'Univers-bulles-La Recherche / oct /2006

[3] *Francis Everitt* - Gravity Probe B Final results of a space experiment to test General Relativity - abstract - Physical Review Letters 2011

[4] *V A Belinski , I M Khalatnikov* -Influence of viscosity on the character of cosmological evolution -J.E.T.P. Soviet Union 13 march1975 pg 205-210

# Thin film deposition using the pulsed laser method

*Phd. Student Lazar Oana Andreea*

In order to achieve multilayer thin films is used technique of pulsed laser deposition (PLD).

Pulsed laser deposition (PLD) is a physical vapor deposition (PVD) technique where a pulsed laser beam is focused inside a vacuum chamber to hit a target of the material that is to be deposited.[1]

The assembly of experimental setup it involves using a laser (Nd:YAG, ArFexcimer), vacuum chamber, target of the material, substrate, gas bottle, turbomolecular pump and a preliminary pump.

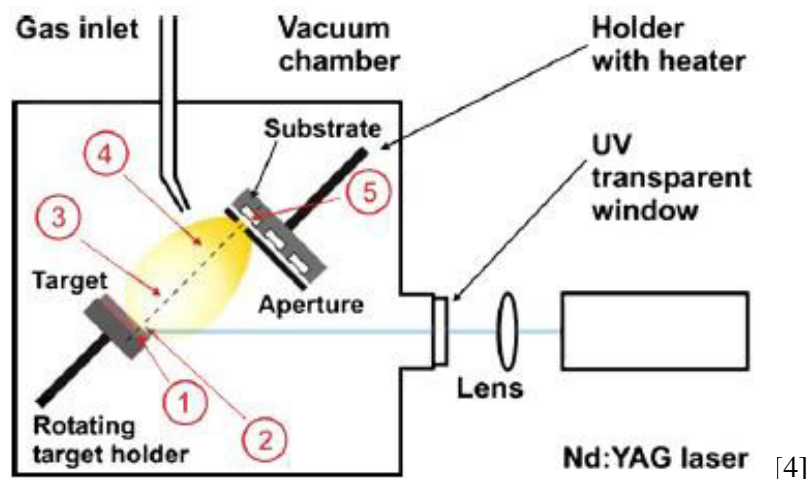
The process of PLD consists of utilizing a pulsed laser beam directed under an angle of  $45^\circ$  towards the target. The target and the substrate are situated in a vacuum chamber at a range of distance from 3 cm to 10 cm. When the pulsed laser beam strikes the target, it's said that occurs the absorbption of photons by the target material.[2]

Therefore, we say than appear the ablation process in which a quantity of material is removed from the target in the form of plasma plume and deposited on the substrate.

When it occurs the phenomena of laser – target interaction, energy is converted to electronic excitation and then into thermal, chemical and mechanical energy.

Thus, it is resulting in evaporation, ablation and plasma plume formation. The plasma plume expands and condenses onto the substrate as thin film.[3]

The operating principle can be seen in the next figure.



The ablation process can occur at atmospheric pressure ( $10^{-2}$  mbar) or in ultra-high vacuum ( $10^{-7}$  –  $10^{-12}$  mbar) in the presence of a background gas (reactive: O<sub>2</sub>, N<sub>2</sub> or inert: Ar, He, Ne). The pressure control is achieved by turbomolecular and preliminary pumps.

Usually, the growth modes of thin films in PLD processes are: step – flow growth, layer – by – layer growth and islands growth. [1]

The growth of multilayer thin films can be influenced by the laser parameters (the fluency and the pulse energy), the background gas pressure (the stoichiometry compounds) and the substrate parameters (temperature).

Consequently, the PLD is a frequently used method which helps to stoichiometric transfer from the target material to the substrate like a thin film.

#### References:

- [1] Robert Eason, “Pulsed laser deposition of thin films: applications – led growth of functional materials”, John Wiley & Sons, Inc, 2007
- [2] Christof W. Scheider, Thomas Lippert, “Chapter 5: Laser Ablation and Thin Film Deposition”, Paul Scherrer Institut
- [3] G. Muller, M. Konijnenberg, G. Krafft, C. Schultheiss, “Science and Technology of Thin Films”, edited by F. C. Matocolta and G. Oltaviani (World Scientific, Singapore, 1995) 89
- [4] J. Schou, Applied Surface Science 255 (2009) 5191 – 5198

## High grade decontamination of Ni targets for sub-barrier transfer reactions

*Andreea Mitu<sup>1,2</sup>, Marius Dumitru<sup>3</sup>, Florian Dumitrache<sup>3</sup>, Nicolae Marginean<sup>1</sup>, Rareş Şuvailă<sup>1</sup>,  
Cristina Niţă<sup>1</sup>, Maria Dinescu<sup>3</sup>, Gheorghe Căta -Danil<sup>2</sup>*

<sup>1</sup>Horia Hulubei-National Institute for Physics and Nuclear Engineering (IFIN-HH), 30 Reactorului Street, 077 125, Magurele, Romania

<sup>2</sup>University Politehnica of Bucharest, 313 Splaiul Independentei, Bucharest, Romania

<sup>3</sup>National Institute for Laser, Plasma and Radiation Physics (INFLPR), 409 Atomistilor Blvd., Magurele, Romania

e-mail: [andreea.mitu@nipne.ro](mailto:andreea.mitu@nipne.ro)

**Keywords:** thermal treatment, sub-barrier transfer reactions

Sub-barrier neutron transfer reactions with  $^{18}\text{O}$  or  $^{13}\text{C}$  have a high spectroscopic potential which has been recently proven in several successful experiments with the RoSPHERE array in Bucharest. However, special care must be provided in this kind of experiments in order to avoid contamination of gamma spectra: if chemical contaminants such as Oxygen are present in the target, the reaction cross-section on these contaminants is much higher than in the case of the reaction of interest.

This work concerns the 2 neutron transfer reaction of  $^{18}\text{O}$  beam on a  $^{64}\text{Ni}$  target at sub-barrier energies. For this experiment were prepared thin ( $\sim 1\text{mg}/\text{cm}^2$ ) and thick ( $\sim 5\text{mg}/\text{cm}^2$ ) metallic layers of  $^{64}\text{Ni}$  with high-purity (99.53% certified enrichment) and with good thickness uniformity on the defined surface. The preparation process started from the metallic powder and followed a series of steps (pressing, heating with an electron-gun and finally rolled), until the required thickness and uniformity were achieved. During the target preparation process, due to the known chemical activity of the Ni powder with the air components, atomic layers of Oxygen are incorporated and also formed on the target surface.

For the experimental energy range, the  $^{18}\text{O}$  beam induced nuclear reactions on the  $^{16}\text{O}$  at the target surface. This is a major drawback, since gamma rays coming from the reactions on  $^{16}\text{O}$  bring a significant contribution in the gamma energy spectrum. In order to overcome it, a thermal treatment with a hydrogen oven was applied.

The performances of the targets after the thermal treatments showed an important reduction of the Oxygen contamination.

# The study of $p$ -Si/TiO<sub>2</sub>/ $n$ -Si (100) sandwiches structures deposited by KrF excimer laser ablation

Calin Moise<sup>1\*</sup>, Alin Jderu<sup>1</sup>, Oana Brincoveanu<sup>1,2</sup>,  
Dionizie Bojin<sup>1</sup>, Marius Enachescu<sup>1</sup>

<sup>1</sup>Center for Surface Science and Nanotechnology, Politehnica University of Bucharest, 060042, Romania

<sup>2</sup>University of Bucharest Faculty of Physics P.O. Box MG-11, Magurele, Ilfov, 077125 Romania  
[\\*calin.moise@cssnt-upb.ro](mailto:calin.moise@cssnt-upb.ro)

**Abstract:** Laser ablation is a versatile technique for deposition of metals, semiconductors as well as dielectrics. Our pulsed laser deposition (PLD) system is set up into an ultra-high vacuum (UHV) machine with working pressure of  $8.5 \cdot 10^{-11}$  Torr. In this work we report the successfully deposition of sandwiches structures  $p$ -Si/TiO<sub>2</sub>/ $n$ -Si (100) substrate. The obtained thin layers were characterized by atomic force microscopy (AFM), scanning electron microscopy (SEM) and composition was investigated by energy dispersive X-ray (EDX). Also micro-Raman spectroscopy was involved for measurement of the stress in  $n$ -Si (100) substrates as well as top deposited  $p$ -Si. The layer thicknesses were measured by ellipsometry technique. Depositions were performed at three different values for: distance between target and substrate (3, 4, 5 [cm]), temperature of substrate (400, 500, 600 [°C]), laser pulse energy (400, 500, 600 [mJ]) and laser pulse repetition rate (20, 30, 40 [Hz]). We conclude that the optimally conditions for both layers deposition are: 5 cm, 500°C, 500mJ, and 30 Hz.

## 1 Introduction

The market demand for thinner field effect transistor (FET), such the 14 nm technology now available, increased the interest of scientists for buried oxides layers. Following this trend we started to deposit successive layers TiO<sub>2</sub> and  $p$ -Si type over  $n$ -Si (100) substrate by laser ablation and to find the proper parameters for uniform surfaces.

Laser ablation is a versatile technique for deposition of: metals, semiconductors as well as dielectrics [1,2].

The TiO<sub>2</sub> is well known insulator with chemical stability even at high temperature, being suitable for thin buried oxide layer.

## 2 Experimental and results

Pulsed laser Deposition (PLD) system is a unique versatile research tool. The system offers a broad range of materials and applications. The ability to extend the vacuum capabilities to ultra-high vacuum base pressures allows the control of unwanted film impurities. Up to now, our best vacuum level is  $8.5 \cdot 10^{-11}$  Torr. The laser target manipulator accommodates up to four 2" diameter wafers which are selectable through the controlling computer. Each of the individual targets can be rotated about its axis, which combined with the laser ablation scanning provides a uniform ablation of the target. Using this flexibility, a multitude of thin film structures deposition are possible.

The system consists of three chambers, load lock, growth and the RHEED gun, which serve for load/unload the targets and samples, deposition and *in-situ* analysis respectively.

The ablations were performed with Coherent Compex pro 205 F KrF excimer laser, having  $\lambda = 248$  nm and pulse duration of 20ns.

First step is the substrate preparation prior to deposition. The commercial (Sigma Aldrich) *n*-Si wafer (100) oriented surface was treated by HF 10% for 10 minutes to eliminate the native oxide from the surface, after being cleaned by acetone and dried in nitrogen flow.

The (100) surface orientation was proved by RHEED investigation (not shown here).

For studying *p*-Si/TiO<sub>2</sub>/*n*-Si (100) sandwiches structures we must have the possibility to investigate both deposited surfaces, therefore after the oxide deposition the samples were taken out and a Ti foil mask was used for partial covering the surface before the deposition of *p*-Si layer [3].

Nanoscale investigations were carried out by AFM (Solver Next) [4,5] and reveal that optimal value of distance, temperature, laser energy, repetition rate are: 4cm, 500□, 500 mJ and 30 Hz respectively for both deposited layers. In Figure 1 are the AFM images for TiO<sub>2</sub> deposited surface. As can be observed the quality of surface is very good (Ra and RMS below 0.6 nm).

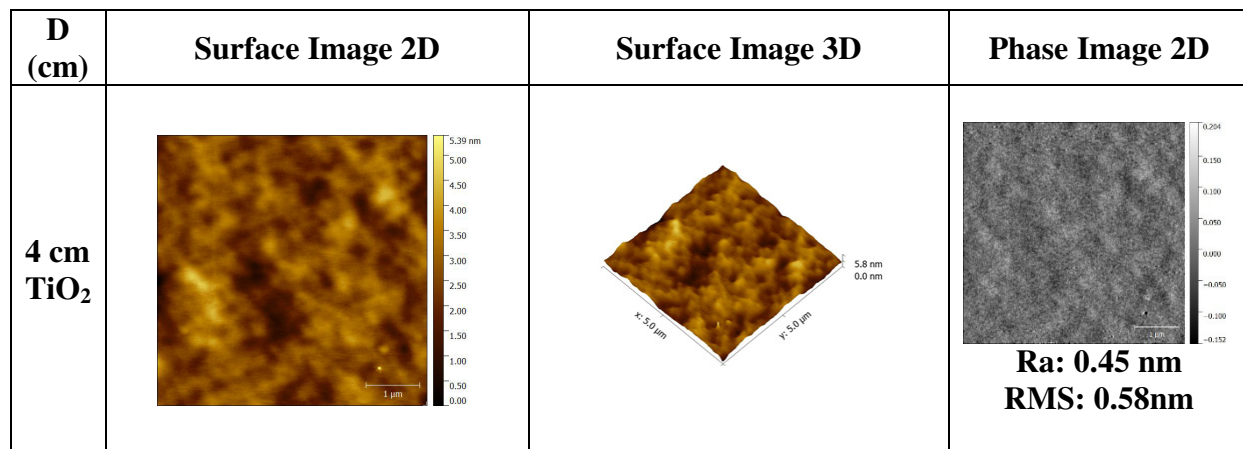


**Figure 1** – AFM images of TiO<sub>2</sub> surface

### 3 Further directions for research

Comparison with sputter deposition technique, measurement of electrical properties of the *p-n* structure modulated by buried TiO<sub>2</sub>.

### 4 References:

- 1) Editor: Phipps Clude “Laser Ablation and its Applications” Springer Series in Optical Science 2007.
- 2) Stafe Mihai, Marcu Aurelian, Puscas Nicolae “Pulsed Laser Ablation of Solids” Springer Series in Surface Science 2014.
- 3) Calin Moise, Oana Brincoveanu, Adrian Katona, Dorel Dorobantu, Dionizie Bojin, Marius Enachescu “The study of *p*-Si/Al<sub>2</sub>O<sub>3</sub>/*n*-Si (100) sandwiches structures deposited by KrF excimer laser ablation” Proceeding of the 40<sup>th</sup>-ARA Montreal Canada 2016.
- 4) A. Moldovan, P.M. Bota, D. Dorobantu, I. Boerasu, D. Bojin, D. Buzatu, M. Enachescu “Wetting properties of glycerol on silicon, native SiO<sub>2</sub>, and bulk SiO<sub>2</sub> by scanning polarization force microscopy” Journal of Adhesion Science and Technology, 28, 13, 1277-1287, (2014).
- 5) A. Moldovan, P.M. Bota, T.D. Poteca, I. Boerasu, D. Bojin, D. Buzatu, M. Enachescu “Scanning polarization force microscopy investigation of contact angle and disjoining pressure of glycerol and sulfuric acid on highly oriented pyrolytic graphite and aluminum” The European Physical Journal Applied Physics, 64, 31302-31308, (2013).

## **New digital acquisition system for a large multichannel spectroscopy array**

**Student: Stan Lucian**

As time passes, more and more nuclei are being investigated, their properties being measured and determined. This creates an incentive for experimenters to develop new detector arrays with more channels and better characteristics. In turn, these modern nuclear experiments necessitate sophisticated multi-channel acquisition systems which can handle and process the large number of signals.

The Nuclear Physics Department of the Romanian National Institute of Nuclear Physics and Engineering in Magurele operates, among others, a 9MV Tandem accelerator. It delivers light nuclei to, among others, the RoSphere detector array, which can receive, in its 25 positions, fast LaBr3 scintillator detectors, HPGe detectors with very good energy resolution and, more recently, neutron detectors. Furthermore, RoSphere has been augmented by the addition of two mobile neutron “walls”, with 12 detectors each.

Besides the addition of neutron detectors, there are plans in the department to expand RoSphere's capacities by adding more ancillary detectors to the set-up, like segmented silicon detectors. However, these plans were hampered by the acquisition system.



*The old RoSphere acquisition system. It's size and impressive number of modules are readily observable. It only recorded signals from 50 channels – Source: Photo taken by the author*

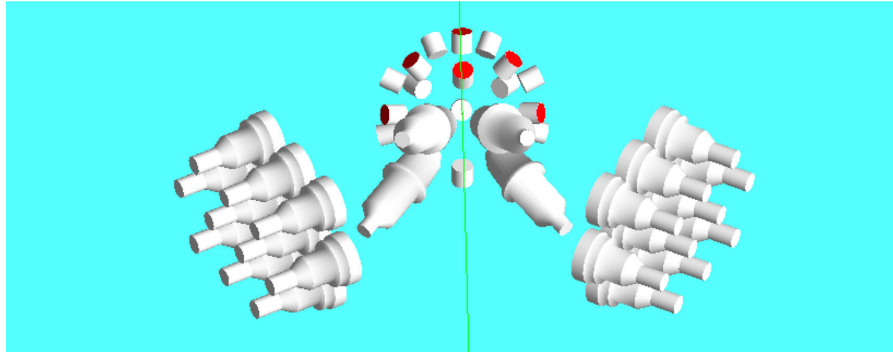
While appreciated as adequate in its role up to that point, it raised significant difficulties if any expansion was to be carried out.

Thus, it was decided to implement a new system, using new state-of-the-art signal processing modules, which would not only allow for the expansion of the RoSphere array, but also bring up many new functionalities. For this system, a control program was developed, based on the open-source Gecko suite written by Bastian Loher.

The new system was ready and commissioned in September 2016. It proved capable of handling the signals from all the 25 detectors of the RoSphere array. Furthermore, new signals have been added. The time and energy from the anti-Compton shields are now recorded, allowing us to employ a multiplicity filter. The energy of the HPGe detectors is registered twice, first with a larger gain,

which allows good energy resolution, and secondly with a smaller gain, which allows us to observe gamma energies of up to 7 MeV.

*A simulation of the RoSphere detector array, as it currently stands, with 10 HPGe detectors, 11*



*LaBr3 detectors and 26 neutron detectors – Source: N. Marginean et al., Spectroscopy and lifetime measurements of low-lying  $T=0, 1$  states in  $^{62}\text{Ga}$ , Proposal for the TANDEM accelerator for the period March 2016 - December 2016*

Recently, at the end of March 2017, neutron detectors were added to the RoSphere array, and the acquisition system had to take in 76 more signals, which it has with ease.

### Images

[1] The old RoSphere acquisition system. It's size and impressive number of modules are readily observable. It only recorded signals from 50 channels – Source: Photo taken by the author

[2] A simulation of the RoSphere detector array, as it currently stands, with 10 HPGe detectors, 11 LaBr3 detectors and 26 neutron detectors – Source: N. Marginean et al., Spectroscopy and lifetime measurements of low-lying  $T=0, 1$  states in  $^{62}\text{Ga}$ , Proposal for the TANDEM accelerator for the period March 2016 - December 2016

### Sources

[1] <http://www.nipne.ro/research/departments/dfn.php>

[2] D. Bucurescu et al / Nuclear Instruments and Methods in Physics Research A 00 (2016)

[3] C. R. NITA et al., Fast-timing lifetime measurements of excited states in  $^{67}\text{Cu}$ , PHYSICAL REVIEW C 89, 064314 (2014)

[4] N. Marginean et al., Measurements of sub-nanosecond nuclear lifetimes with an array of HPGe and LaBr3 detectors, Eur. Phys. J. A 46, 329336 (2010)

[5] <http://www.mesytec.com/products/datasheets/MSCF16-LN.pdf>

[6] <http://www.mesytec.com/products/datasheets/MADC-32.pdf>

[7] <http://www.mesytec.com/products/datasheets/MTDC-32.pdf>

[8] <http://www.struck.de/pcivme.htm> [14] Ortec: Electronic Standards and Definitions, [www.ortec-online.com/download/electronics-standards-definitions.pdf](http://www.ortec-online.com/download/electronics-standards-definitions.pdf)

[9] <http://www.wiener-d.com/sc/powerd-crates/vme/>

[10] <http://www.osti.gov/scitech/biblio/7120327>

[11] The defunct ESONE website <https://esone.web.cern.ch/ESONE/>

[12] [http://pinouts.ru/Slots/vmebus\\_pinout.shtml](http://pinouts.ru/Slots/vmebus_pinout.shtml)

[13] Gamma-ray spectroscopy with a LaBr3 : (Ce) scintillation detector at ultra high count rates, Master thesis, Bastian Lher, November 2010, [http://www.ldot.de/mediawiki/images/Master\\_thesis.pdf](http://www.ldot.de/mediawiki/images/Master_thesis.pdf)

[14] <http://www.gnu.org/licenses/lgpl-3.0.en.html>

[15] N. Marginean et al., Spectroscopy and lifetime measurements of low-lying  $T=0, 1$  states in  $^{62}\text{Ga}$ , Proposal for the TANDEM accelerator for the period March 2016 - December 2016

[16] <http://www.sparrowcorp.com/downloads/kmax-9-0>

[17] A. Turturica, Private Communication

# Assessment of a Hybrid Acquisition System for Positron Annihilation-based Spectroscopy

Sebastian Toma<sup>1,2</sup>

<sup>1</sup> PhD student, Faculty of Applied Sciences, University POLITEHNICA of Bucharest, Romania

<sup>2</sup> Department of Nuclear Physics, “Horia Hulubei” National Institute for Physics and Nuclear Engineering, Măgurele, Romania

*A hybrid (digital and analogic) data acquisition system for Positron Annihilation Spectroscopy is described. Results of comparative testing measurements using pairs of the same HPGe detectors using both purely digital and analogic setups reported*

## 1. Introduction

Positron Annihilation Spectroscopy (PAS) is a class of non-destructive techniques used for materials testing, based on the implantation of positrons from radioactive sources into the samples and followed by measurements of the annihilation characteristics. These characteristics are strongly influenced by trapping of positrons in vacancy-type defects and thus make the PAS excellent tools for defects detection (dislocations, vacancies, clusters) in the material microstructure. The LaMAR laboratory at Politehnica University uses two methods of PAS technique: Positron Annihilation Lifetime Spectroscopy (PALS) and Coincidence Doppler Broadening Spectroscopy (CDBS) currently implemented in a classical manner (i.e. analogic measurement chain).

## 2. Experimental Setups

The two methods already available at LaMAR are:

1. Positron annihilation lifetime spectroscopy (PALS). Details on the turn-key system can be seen in [1] and [2].
2. Coincidence Doppler Broadening Spectroscopy (CDBS): This method exploits the lineshape of the 511 keV annihilation gamma-rays. [3].

Given the advent of digitizers [4], data acquisition systems can be simplified while at the same time offer more flexibility in treating the recorded data. In the past decade, a series of digital spectrometers for PAS have been developed [3][5][6], making use of the *waveform-mode* of operation, with offline treatment of the *raw data*.

The XIA DGF4C rev.F digitizers used in the present work are designed for operating with HPGe detectors by internal FPGA *filtering and shaping* of the raw preamplifier signals, while also providing an *integration* mode of operation.

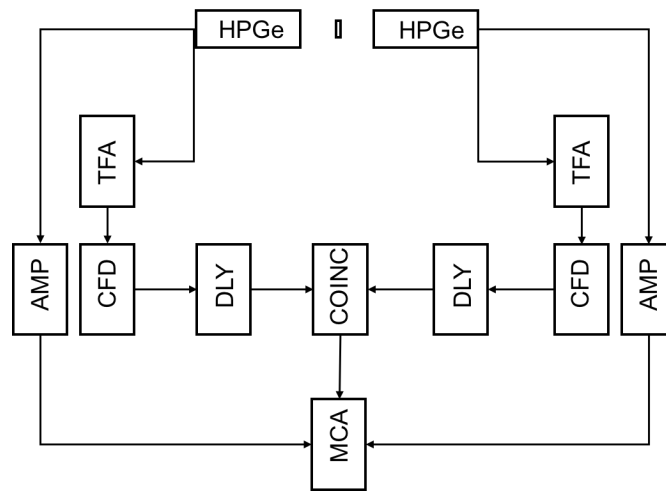


Fig. 1 – Block-diagram of the analogic CDBS system

In effect, this eliminates the need for preprocessing HPGe signals. The drawback is the low sampling rate, making the typical timing resolutions required for lifetime measurements unachievable without extra modules. Thus, a hybrid system has been set up (Figure 2).

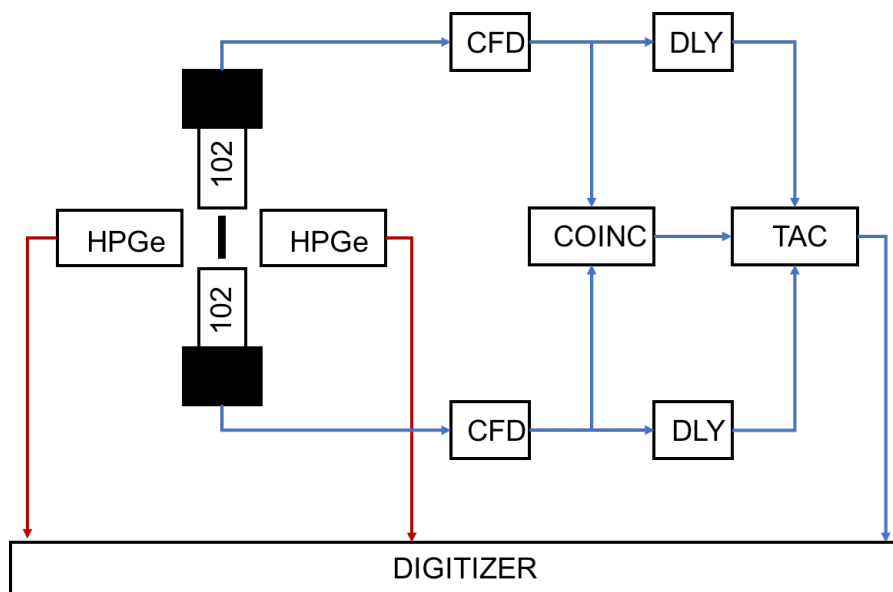


Figure 2 – Block-diagram of the Hybrid system. Both PALS and CDBS can be run simultaneously. [red] HPGe preamp signals fed directly to the digitizer. [blue] analogic pre-processing for PALS

### 3. References

- [1] Paulus, T.J. – China Nuclear Society Seminar, Beijing, China, 1995
- [2] PLS-System – Positron Lifetime Picosecond Timing System Datasheet, <http://www.ortec-online.com>
- [3] Cizek, A – NIM A 623 (2010) 982-994
- [4] Warburton, W.K. – Appl. Radiat. Isot. 2000 Oct; 53(4-5):913-20
- [5] Nissila, J. – NIM A 538 (2005) 778-789
- [6] Becvar, F. – NIM A 539 (2005) 372-385

**Session MATHEMATICS**  
**abstracts**

# IMPLICATIONS OF RANDOM PROCESSES THEORY BY MS EXCEL AND ORIGIN IN THE STUDY OF LINEAR DYNAMIC SYSTEMS

Bogdan CIORUȚA<sup>1,3</sup>, Nicolae POP<sup>2</sup>, Tudor SIRETEANU<sup>2,3</sup>

<sup>1</sup>North University Centre at Baia Mare - Technical University of Cluj-Napoca, Faculty of Engineering  
Victor Babeș str., no. 62A, 430083, Baia Mare  
[bciorutza@yahoo.com](mailto:bciorutza@yahoo.com)

<sup>2</sup>Institute of Solid Mechanics of the Romanian Academy  
Constantin Mille str., no. 15, sector 1, Bucharest

<sup>3</sup>University Politehnica of Bucharest - Faculty of Applied Sciences  
Splaiul Independenței, no. 313, RO-060042, sector 6, Bucharest

## Abstract (ro):

Since ancient times, the phenomena of nature and society were present in people's daily scientific activities, and as society evolved, their importance in the complex system of human civilization has steadily increased. The study of nature and society was led scientists to create theories and mathematical models that include the main characteristics of abstract forms. For the phenomena of nature and society, which are originally evolutionary phenomena (dynamic), the best model was found to be the result of specific observation and measurement-based methods, concepts at the core of natural and technical sciences.

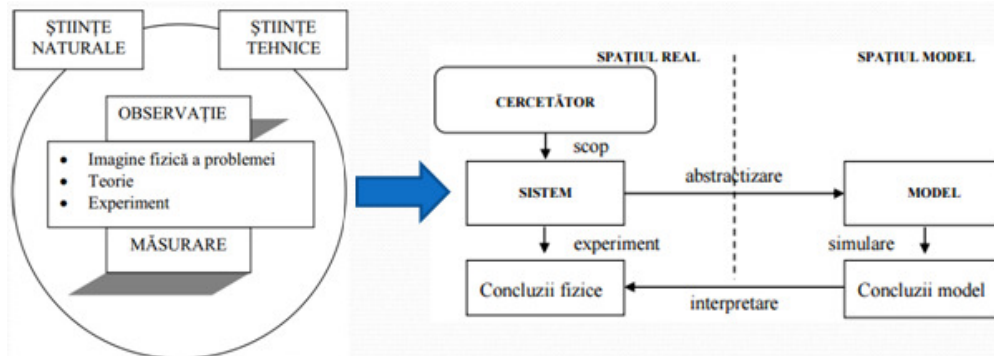


Figure 1. Position of the measurement and evaluation concepts in relation to natural and technical sciences

The main purpose of dynamical systems theory, which we have raised, is to understand the long-term behavior of states of a system, most often deterministic. For this study, we follow, from concepts specific systems theory, achieving a ranking non-exhaustive patterns or systems, depending on the linearity, of their number of input-output variables, of behavior over time or taking into account other aspects. Often, such systems involve many variables and are nonlinear. Therefore, the study of the behavior of dynamic systems require graphics (modeling and simulation) particularly complex that can be easily done with computers from nowadays, some of them will be presented in the paper.

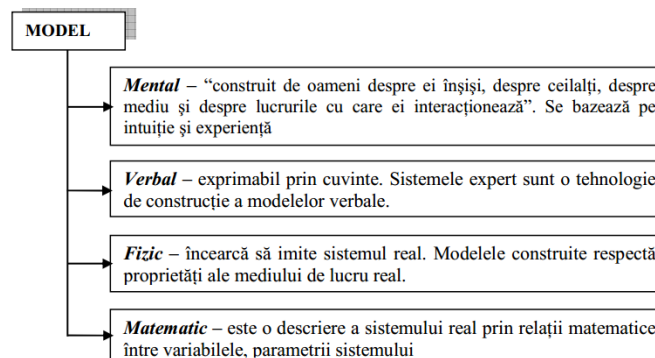


Figure 2. Various models and their representation

	Sisteme liniare	Sisteme neliniare	Tipul de model	Caracterizare
1			Modele utilizate în scopul cercetării Modele utilizate în management Modele deterministe	utilizate ca un instrument de cercetare utilizate ca un instrument de management valorile prezise au valoare generată exact depind numai de datele de intrare
2	Sisteme continue Sisteme discrete		Modele stocastice	valorile prezise depind de distribuții probabilistice
3	Sisteme deterministe Sisteme nedeterministe		Modele reduționiste Modele holiste Modele statice	includ pe cât posibil toate detaliile relevante utilizează principii generale
4	Sisteme cu parametrii concentrați Sisteme cu parametrii distribuiți		Modele dinamice Modele distributive	variabilele care definesc sistemul nu sunt dependente de timp variabilele care definesc sistemul sunt funcții de timp sau spațiu
5	Sisteme invariabile în timp Sisteme variabile în timp		Modele agregative (engl. "lumped")	parametrii sunt considerați funcții de timp și spațiu
6	Sisteme cauzale		Modele liniare Modele neliniare Modele de cauzalitate	definite la scară spațială mare, exprimate prin valori medii ale variabilelor de stare și proces considerate ecuații de gradul I una/mai multe ecuații nu sunt de gradul I, ecuații de grad superior sau funcții neliniare
7	Sisteme stabile Sisteme instabile		Modele necauzale (engl. "black-box") Modele autonome/independente	intrările, variabilele de stare, ieșirile sunt interrelaționate prin relații de cauzalitate intrările în sistem sunt comparate cu ieșirile fără analiza mecanismului intern cauzal
8	Sisteme monovariabile Sisteme multivariabile		Modele dependente	derivatele nu sunt în mod explicit dependente de variabila independentă (timpul) derivatele sunt în mod explicit dependente de variabila independentă (timpul)

Figure 3. Types of physical (real) systems and associated models

The fundamental feature of dynamic systems involving the movement and the objective existence in time and space of physical systems they set up purely mathematical, as mature fruits of researchers thought.

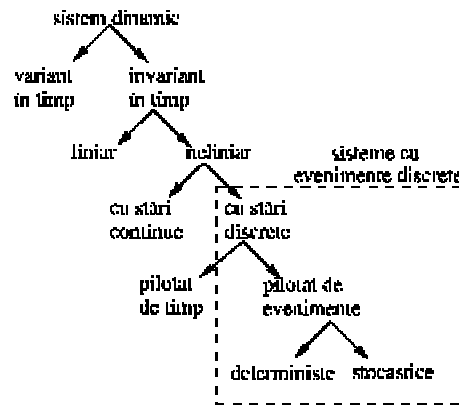


Figure 4. Overall classification of dynamic mechanical systems

The study of natural systems and processes is based on the causality principle; physical systems shows mechanical, thermal, electrical and magnetic properties, which can be analyzed in successive stages.

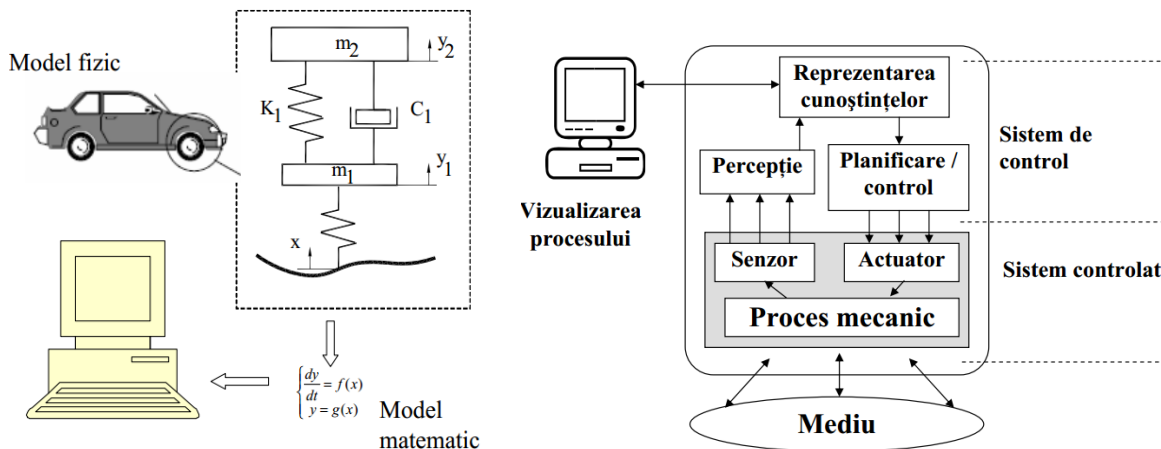
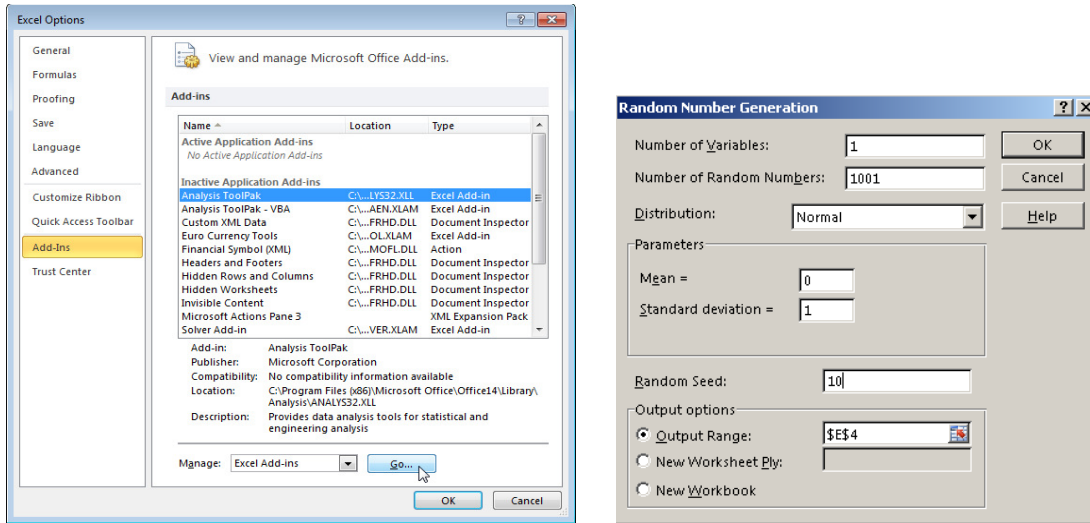


Figure 5. Specific steps in the systemic analysis methodology and behavior control

Considering the stated, the present study shows, in addition to the above mentions, concepts which have a significant role in the study of linear dynamic systems, from the random processes theory perspective, among which we considered the distribution function, density function of probability, statistical moments of a random process, and the correlation (cross-correlation) of a random signal (process). A special place is allocated, towards the end, to the methodology that generates and analyzes the random sets of data (variables) through the software readily available, namely, MS Excel, respectively Origin.



Parameters	random seed	time (t)										
		10	20	30	40	50	60	70	80	90	100	
mean	0	0	-2.85283	-2.73241	-2.63957	-2.56507	-2.50431	-2.45007	-2.40219	-2.3605	-2.32141	-2.28558
st. deviation	1	0.01	0.03944	0.82704	-1.43235	-0.36868	0.3487	1.38192	-0.85361	-0.05813	0.69663	-1.78525
		0.02	-1.28237	0.12961	-2.71986	-0.11304	1.32073	-0.36271	0.87843	-0.63766	0.5638	-0.97308
		0.03	-0.20722	0.71103	-1.25366	-0.12937	0.81365	-1.10033	-0.05223	0.92577	-0.96915	0.02452
		0.04	-0.20698	0.16557	0.5637	1.08615	-2.36425	-1.00781	-0.51137	-0.11981	0.25349	0.66766
		0.05	0.14683	0.69575	1.69621	-1.02202	-0.38067	0.1259	0.66958	1.61436	-1.05762	-0.40305
		0.06	-0.82338	-1.01533	-1.2545	-1.80127	-2.6108	1.68884	1.30605	1.05401	0.8557	0.68633
		0.07	-1.32901	-0.84658	-0.50928	-0.22256	0.04672	0.31941	0.61874	0.98879	1.60099	-1.6263
		0.08	-0.36418	-0.26163	-0.16177	-0.0635	0.03416	0.13207	0.23135	0.33297	0.43815	0.54844
		0.09	-1.57218	-0.90876	-0.50867	-0.1783	0.13331	0.45871	0.84352	1.43471	-1.6642	-0.94712
		0.1	-1.11005	-1.35098	-1.71454	2.89561	1.67437	1.32753	1.09252	0.90611	0.74685	0.60453
		0.11	1.13127	1.19757	1.26976	1.34908	1.43814	1.54009	1.66146	1.81343	2.02519	2.40911
		0.12	0.81035	0.11904	-0.51399	-1.55606	0.9007	0.18242	-0.44372	-1.37322	0.99908	0.24654
		0.13	-1.57086	-1.23918	-1.00603	-0.81781	-0.65491	-0.5078	-0.3709	-0.24071	-0.1145	0.00991
		0.14	-0.25523	-0.94724	1.59197	0.57342	-0.02682	-0.63775	-1.82101	0.86634	0.20027	-0.38034
		0.15	0.76231	-1.48927	-0.36018	0.38676	1.56929	-0.72947	0.06028	0.89726	-1.24614	-0.25974
		0.16	-0.1075	0.36214	0.93687	-2.33522	-0.86334	-0.31025	0.15704	0.66384	1.48189	-1.20039
		0.17	-0.18888	-1.66451	0.44262	-0.54205	1.38411	0.0998	-0.98345	0.79138	-0.23127	-1.85969
		0.18	0.38577	-0.81046	0.73077	-0.4504	1.20008	-0.14181	-2.83537	0.15348	-1.17667	0.46322
		0.19	0.32433	0.86445	2.18359	-0.97566	-0.40214	0.0576	0.53056	1.18142	-1.5512	-0.70759
		0.2	-1.15583	0.27313	-1.33254	0.18935	-1.56485	0.10688	-1.93858	0.02513	2.49907	-0.05645
		0.21	0.51766	-0.1966	-0.05174	1.13054	0.24118	-0.46859	-1.70498	0.73397	-0.01779	-0.78127
		0.22	-0.69663	0.93544	-0.23434	2.30913	0.18071	-1.02009	0.63111	-0.47266	1.28359	-0.04389
		0.23	1.48556	-1.46133	-0.79725	-0.37631	-0.01496	0.34439	0.7568	1.37934	-1.58253	-0.85075
		0.24	-2.05903	-0.05959	1.49649	-0.28148	1.01803	-0.51828	0.7019	-0.78897	0.44422	-1.13578
		0.25	-0.21402	0.80685	-0.97418	0.10011	1.37068	-0.55449	0.42472	-1.75842	-0.21668	0.80336

	$x_1(t)$	$x_2(t)$	$x_3(t)$	$x_4(t)$	$x_5(t)$	$x_6(t)$	$x_7(t)$	$x_8(t)$	$x_9(t)$	$x_{10}(t)$
Mean	-2.8528	-2.7324	-2.6396	-2.5651	-2.5043	-2.4501	-2.4022	-2.3605	-2.3214	-2.2856
Standard Error	0.04678	-0.0423	-0.0672	0.02098	-0.0116	0.01632	-0.0206	0.04155	0.02523	-0.0601
Median	0.03234	0.03215	0.03132	0.03112	0.03101	0.03108	0.03087	0.03139	0.03179	0.03067
Mode	0.06334	-0.0583	-0.0833	0.00298	-0.0158	0.05269	-0.0142	0.02961	0.06952	-0.0726
Skewness	0.73808	0.69575	-2.7199	-0.9981	1.67437	-0.6377	0.82145	-0.1905	0.54214	-0.3902
Standard Deviation	1.02277	1.01671	0.99056	0.98421	0.98069	0.9827	0.97611	0.99268	1.00525	0.96997
Sample Variance	1.04606	1.03371	0.98122	0.96866	0.96175	0.96569	0.9528	0.98542	1.01052	0.94083
Kurtosis	-0.0108	0.05151	-0.0444	-0.2903	0.20504	-0.0606	-0.2462	-0.1489	-0.3353	0.00053
Skewness	-0.072	-0.0523	-0.0098	0.10834	-0.0759	-0.0267	-0.0267	-0.0681	-0.1133	0.17731
Range	6.32601	6.833	6.33086	5.39076	6.89994	6.43078	5.86595	6.83794	5.74131	6.3538
Minimum	-3.046	-3.4558	-3.6682	-2.3821	-3.5227	-3.4558	-2.9948	-3.3152	-3.1067	-2.8311
Maximum	3.28	3.7721	2.66271	3.00861	3.37721	2.97499	2.87117	3.52273	2.63462	3.52273
Sum	46.7815	-42.255	-67.178	20.9776	-11.619	16.3186	-20.591	41.5499	25.2257	-60.053
Count	1000	1000	1000	1000	1000	1000	1000	1000	1000	1000

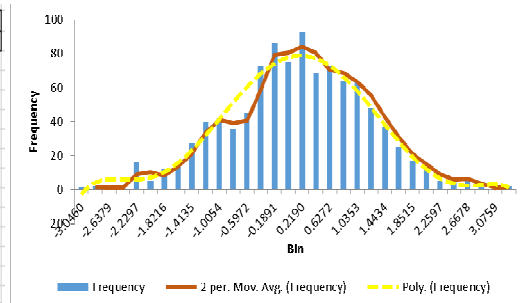


Figure 6. The normal distribution generation, in relation to given average and standard deviation data, of some random data sets, using Data Analysis package –Random Number Generation module

Keywords: dynamic systems, random variables, Analysis ToolPak, Origin.

## LIST OF REFERENCES (SELECTIVE BIBLIOGRAPHY)

- [1]. Cîrtoaje V., (2012) *Introducere în teoria sistemelor - note de curs*, Facultatea de Inginerie Mecanică și Electrică, Universitatea Petrol-Gaze din Ploiești [ac.upg-ploiesti.ro/cursuri/ts/curs\\_ts.pdf](http://ac.upg-ploiesti.ro/cursuri/ts/curs_ts.pdf)
- [2]. Dolga V., (2013) *Teoria sistemelor automate - note de curs, Cap. 2 - Sisteme: definiții și evoluție*, Facultatea de Inginerie Mecanică, Univ. Politehnică din Timișoara [www.mec.upt.ro/dolga/cap\\_2.pdf](http://www.mec.upt.ro/dolga/cap_2.pdf)
- [3]. Dumitrașcu V., (2006) *Abordarea sistemică - instrument al managementului complexității*, Theoretical and Applied Economics, (2):77-82 <http://store.ectap.ro/articole/41.pdf>
- [4]. Gillman M., (2009) *An Introduction to Mathematical Models* (2<sup>nd</sup> Ed.), Wiley-Blackwell, USA
- [5]. Hodgkin L., (2005) *A History of Mathematics: From Mesopotamia to Modernity*, Oxford University Press Inc., New York - [hmath-cs.aut.ac.ir/A\\_History\\_of\\_Mathematics...pdf](http://math-cs.aut.ac.ir/A_History_of_Mathematics...pdf)
- [6]. Jackson L., Trebitz A., (2000) *An Introduction to the Practice of Modeling*, BioScience, USA
- [7]. Katz V., (2009) *A history of mathematics*, Pearson Ed. Inc., USA - [deti-bilingual.com/Mathematics.pdf](http://deti-bilingual.com/Mathematics.pdf)
- [8]. Mahalu G., Pentiu R., (2014) *Abordarea logistică a sistemelor dinamice neliniare*, Conferința internațională – "Prof. D. Pavel - fondatorul hidroenergeticii românești", Sebeș <http://stiintasiinginerie.ro/26-30.pdf>
- [9]. Păun M., (2010) *Bazele analizei de sistem, Cap. 1 - Analiza sistemelor - obiect de studiu și metode de investigare*, Academia de Studii Economice, București [www.asecib.ase.ro/Paun/cuprins.html](http://www.asecib.ase.ro/Paun/cuprins.html)
- [10]. Sireteanu T., (1981) *Sisteme mecanice oscilante neliniare supuse la oscilații aleatoare* (teza de doctorat), Institutul Central de Fizică, București
- [11]. Thelen E., (2005) *Dynamic Systems Theories*, University of California [www.iub.edu](http://www.iub.edu)
- [12]. Vertan C., Gavăț R., Stoian R., (1999) *Variabile și procese aleatoare: principii și aplicații*, Ed. Printech, București
- [13]. "Analiza spectrală a semnalelor aleatoare" - [www.tc.etc.upt.ro/analiza\\_spectrala.pdf](http://www.tc.etc.upt.ro/analiza_spectrala.pdf)
- [14]. "Probabilități și statistică" - [civile.utcb.ro/cmat/cursrt/psvp.pdf](http://civile.utcb.ro/cmat/cursrt/psvp.pdf)
- [15]. "Procese aleatoare" - [alpha.imag.pub.ro/ro/cursuri/tti2/procal.pdf](http://alpha.imag.pub.ro/ro/cursuri/tti2/procal.pdf)
- [16]. "Semnale aleatoare" - [telecom.etc.tuiasi.ro/.../semnale\\_aleatoare.pdf](http://telecom.etc.tuiasi.ro/.../semnale_aleatoare.pdf)
- [17]. "Teoria probabilităților" - [math.etti.tuiasi.ro/lpopa/cursTP.pdf](http://math.etti.tuiasi.ro/lpopa/cursTP.pdf)
- [18]. "Variabile aleatoare" – [analizamatematicapt/.../cap6pdf.pdf](http://analizamatematicapt/.../cap6pdf.pdf) / [math.ubbcluj.ro](http://math.ubbcluj.ro)
- [19]. "Variabile aleatoare și funcții de repartiție" - [www.cermi.utcluj.ro/doc/Cap\\_4.pdf](http://www.cermi.utcluj.ro/doc/Cap_4.pdf)
- [20]. "Variabile și procese aleatoare: principii și aplicații" – [www.miv.ro/.../vpa.pdf](http://www.miv.ro/.../vpa.pdf)
- [21]. <https://ro.wikipedia.org/wiki/...> (Teoria sistemelor, Dynamical systems theory, Deterministic system, Modelul unui sistem, Proces stochastic, Variabile aleatoare etc).

# A FUNCTIONAL EQUATION OF BUTLER-RASSIAS TYPE AND ITS HYERS-ULAM STABILITY

MONEA MIHAI

The aim of this paper is to solve a trigonometric functional equation of Butler-Rassias type and its pexiderized version. Some Hyers-Ulam stability results are also stated.

We will present some results concerning the solution as well as the Hyers-Ulam stability of the functional equation

$$f(x+y) = af(x)\cos y + bf(y)\cos x,$$

where  $f : \mathbb{R} \rightarrow \mathbb{R}$  and  $a, b$  are real parameters. Such type of functional equations that define well-known functions, or classical trigonometric formulas were studied by many authors. Our functional equation in case  $a = b = 1$  is the equation defining the sine function, modulo a real constant  $c$ , as we can see in the sequel. In this case, the following trigonometric formula is obtained:

$$\sin(x+y) = \sin x \cos y + \cos x \sin y.$$

Following the published works of a number of mathematicians such equations are known as Butler – Rassias equations.

In the final section we study the following pexiderized equation:

$$f(x+y) = ag(x)\cos y + bh(y)\cos x,$$

where  $f, g, h : \mathbb{R} \rightarrow \mathbb{R}$  and  $a, b$  are any nonzero real numbers.

## REFERENCES

- [1] S. Butler, *Problem no. 11030*, Amer. Math. Monthly 110 (2003), 637-637.
- [2] D. H. Hyers, *On the stability of the linear functional equation*, Proc. Natl. Acad. Sci. U.S.A. 27 (1941), 222-224.
- [3] S.-M. Jung, *Hyers-Ulam stability of Butler-Rassias functional equation*, J. Inequal. Appl. 2005 (2005), 41-47.
- [4] S. – M. Jung, M. Th. Rassias and C. Mortici, *On a functional equation of trigonometric type*, Applied Mathematics and Computation, 252 (2015), 294 – 303.
- [5] S.-M. Jung, *Hyers-Ulam-Rassias Stability of Functional Equations in Nonlinear Analysis*, Springer Optimization and Its Applications Vol. 48, Springer, New York, 2011.
- [6] S.-M. Jung and B. Chung, *Remarks on Hyers-Ulam stability of Butler-Rassias functional equation*, Dyn. Contin. Discrete Impuls. Syst. Ser. A Math. Anal. 13 (2006), no. 2, 193-197.
- [7] H.-M. Kima and I.-S. Chang, *Approximate linear derivations and functional inequalities with applications*, Appl. Math. Lett. 25 (2012) 830-836.
- [8] C. Mortici, M. Th. Rassias and S.-M. Jung, *On the stability of a functional equation associated with the Fibonacci numbers*, Abstract Appl. Anal. 2014 (2014), Article ID 546046.
- [9] C. Mortici, M. Th. Rassias and S.-M. Jung, *The inhomogeneous Euler equation and its Hyers-Ulam stability*, Applied Mathematics Letters 40 (2015), 23-28.
- [10] M. Th. Rassias, *Solution of a functional equation problem of Steven Butler*, Octagon Math. Mag. 12 (2004), 152-153.
- [11] S.-E. Takahasi, T. Miura and H. Takagi, *Exponential type functional equation and its Hyers-Ulam stability*, J. Math. Anal. Appl. 329 (2007), 1191-1203.
- [12] S. M. Ulam, *Problems in Modern Mathematics*, Chapter VI, Science Editions, Wiley, New York, 1964.

UNIVERSITY POLITEHNICA OF BUCHAREST  
E-mail address: mihaimonea@yahoo.com

# Hydraulic servomechanism models with delay

Daniela Enciu<sup>1,2</sup>, Andrei Halanay<sup>2</sup>, Ioan Ursu<sup>2</sup>

<sup>1</sup>National Institute for Aerospace Research “Elie Carafoli” – INCAS,  
Bd. Iuliu Maniu 220, Bucharest 061126, Romania

<sup>2</sup>University Politehnica of Bucharest, Mathematics Department 2,  
Splaiul Independentei 313, Bucharest 060042, Romania

The problem of modelling hydraulic servomechanisms as systems with delay is relative new, although the delay is objective and real in every system. Probably this situation is given by the difficulties that can be encountered in modelling a state delay as derived from specific nonlinearities like dry friction in hydraulic cylinder. This direction may seem less natural than the introduction of the delay due to a physical law, such as the speed of propagation of a wave, for example, in the case of other systems.

The objective of this paper is to set both of a state of the art in the domain of hydraulic servomechanisms and introducing state delays as a technique for simplifying the model in the view of a qualitative study of the effects of the delay. The hydraulic servomechanism (mechanical or electrical) is an automatic system. Therefore two possible “locations” for the delay are taken into account: on state and on control.

In the specialty literature, in recent years, interest has emerged for assimilating the LuGre friction model with a delayed state model. An older approach is due to V. A. Hohlov where the nonlinear term from the mathematical model of the servomechanism flow equation is replaced with a state-delay. The delay on the control is justified and unavoidable in every automatic system. Often, the delay coming from the sensors is studied. The signal sampling, as usual procedure for elaborating and implementing control laws, also introduces delays in the systems as well. The compensation techniques of the delay effects are multiple and are studied in both time and frequency domain. One technique is the Smith predictor.

The paper ends with a few conclusions regarding the objectives of future studies in the mathematical modelling of the hydraulic systems with state and/or control delays.

# Stochastic connectivity on almost-Riemannian structures induced by symmetric polynomials

Teodor Țurcanu, Constantin Udriște

## 1 Short presentation

In this paper we introduce an almost-Riemannian structure which is induced by the exact differential 1-forms  $\omega_1 = dx + dy$ ,  $\omega_2 = ydx + xdy$ . These are obtained by taking the differential of the elementary symmetric polynomials, defined on the real plane  $\mathbb{R}^2$ , endowed with the coordinates  $(x, y)$ . Clearly, the given 1-forms are functionally dependent on the set  $\{x = y\}$  and functionally independent elsewhere. The kernels of the 1-forms  $\omega_1$  and  $\omega_2$  are generated by the vector fields

$$X_1 = \partial_x - \partial_y \text{ and } X_2 = x\partial_x - y\partial_y,$$

respectively, which span the distribution  $\mathcal{D} = \text{span}\{X_1, X_2\}$ , inducing an almost-Riemannian structure on  $\mathbb{R}^2$ . The *singular locus*, i.e., the set of points at which the vector fields  $X_1$  and  $X_2$  lose their linear independence, is the set  $S = \{(x, y) \in \mathbb{R}^2 \mid x = y\}$ .

The sub-Riemannian metric  $g$ , which turns the pair  $\{X_1, X_2\}$  into an orthonormal basis at each point  $p \in \mathbb{R}^2 \setminus S$ , is given by

$$g = (g_{ij}) = \frac{1}{(x-y)^2} \begin{pmatrix} 1+y^2 & 1+xy \\ 1+xy & 1+x^2 \end{pmatrix}, \quad (1)$$

and clearly is singular on  $S$ .

The almost-Riemannian structure defined above resembles, in some aspects, the famous (in the context of sub-Riemannian geometry) Grushin plane (with the structure induced by the vector fields  $\partial_x, x\partial_y$ ) studied by many authors (see for instance [1, 3, 4, 8, 9]) from various viewpoints.

Recall that, given a smooth manifold  $M$ , a sub-Riemannian structure on  $M$  is specified by a given distribution  $\mathcal{D}$ , i.e., a sub-bundle  $\mathcal{D} \subseteq TM$ , together with a metric  $g$  defined on  $\mathcal{D} \times \mathcal{D}$ . Most often, the distribution is specified by a family of vector fields and is non-integrable.

The natural curves on sub-Riemannian manifolds are *horizontal (admissible) curves*, which are tangent to horizontal vectors. Thus, a classical problem, in the context of sub-Riemannian geometry, is to join two arbitrary points by admissible curves. A sufficient condition for this to be possible is that the vector fields, together with their iterated Lie brackets span the entire tangent space at each point  $p \in M$ . This fact is established by the famous Chow-Rashevskii Theorem [10, 14].

It is easily verified that, in this case, the bracket generating condition is satisfied:

$$[X_1, X_2] = \partial_x + \partial_y,$$

i.e., the Carnot-Carathéodory distance  $d_C$  between any two points is finite, moreover, the topology induced by the metric  $d_C$  is equivalent to the Euclidean topology (Corollary 2.6 [3]).

In this paper we are interested in stochastic analogues of connectivity problems on almost-Riemannian manifolds. To our knowledge, this problem was raised and motivated, for an arbitrary sub-Riemannian manifold, in [6, 7]. The problem has been solved for the Grushin plane and its generalizations in [6, 7, 16, 17, 18]. The main result of the paper is Theorem 1.2, which proves the stochastic connectivity property with respect to the almost-Riemannian structure defined above.

It is worth mentioning that when passing to a stochastic setting some important adjustments need to be made. Firstly, the admissible curves are replaced by *admissible stochastic processes* (defined below). Secondly, we have to replace the deterministic boundary conditions as well, since probability of an admissible stochastic process, starting at a state  $P$ , to reach a fixed state  $Q$ , is zero. Thus, we ask for a time at which the state of the process is in an arbitrarily small neighborhood of the state  $Q$ , with the probability close enough to one.

Any admissible curve  $c : [0, T] \rightarrow \mathbb{R}^2$ , between two fixed points  $P$  and  $Q$  is described by the boundary value problem

$$\begin{cases} dx(t) = [u_1(t) + u_2(t)x(t)] dt \\ dy(t) = -[u_1(t) + u_2(t)y(t)] dt \\ (x(0), y(0)) = (x_P, y_P), \quad (x(T), y(T)) = (x_Q, y_Q), \end{cases} \quad (2)$$

for some control functions  $u_1, u_2 \in L^1([0, T], \mathbb{R})$ . Using a pair of independent Wiener processes  $(W_t^1, W_t^2)$ , together with a pair of nonnegative constants  $(\sigma_1, \sigma_2)$ , the ODE system (2) is stochastically perturbed, yielding the SDE system

$$\begin{cases} dx(t) = [u_1(t) + u_2(t)x(t)] dt + \sigma_1 dW_t^1 \\ dy(t) = -[u_1(t) + u_2(t)y(t)] dt + \sigma_2 dW_t^2. \end{cases} \quad (3)$$

Here the controls  $u_i(s) = u_i(s, \omega)$ ,  $i = 1, 2$  are stochastic processes measurable with respect to the  $\sigma$ -algebra generated by  $\{W_{s \wedge t}, t \geq 0\}$ , taking values in a Borel set at any instant. The controls which do not depend on  $\omega$  are called *deterministic* or *open loop controls*. Controls of the form  $u(s, \omega) = u_0(t, c_t(\omega))$ , for some function  $u_0$ , are called *Markov controls*. Denote the set of deterministic controls by  $\mathcal{U}_1$  and, respectively, the set of Markov controls by  $\mathcal{U}_2$ .

**Definition 1.1.** A stochastic process  $c_t = (x(t), y(t))$  solving the SDE system (3) is called *admissible stochastic process*.

**Theorem 1.2.** Let  $P(x_P, y_P)$  and  $Q(x_Q, y_Q)$  be two given points on  $\mathbb{R}^2$  and denote by  $D_C(Q, r)$  the Carnot-Carathéodory disk of radius  $r$  centered at  $Q$ . Then, for any  $\varepsilon \in (0, 1)$  and  $r > 0$ , there exist an admissible stochastic process  $c_t = (x(t), y(t))$ , and a striking time  $T < \infty$ , such that

$$\mathbb{P}[c_T \in D_C(Q, r)] \geq 1 - \varepsilon, \quad (4)$$

and  $x(0) = x_P$ ,  $y(0) = y_P$ ,  $\mathbb{E}[y(T)] = y_Q$ ,  $\mathbb{E}[x(T)] = x_Q$ .

## 2 A three dimensional generalization

In the present section we discuss a generalization of previously obtained result in a three-dimensional setting, i.e., on  $\mathbb{R}^3$  with the usual coordinates  $(x, y, z)$ . Taking the differential of the symmetric polynomials  $s_1 = x + y + z$ ,  $s_2 = xy + yz + zx$  and  $s_3 = xyz$ , respectively, we obtain the differential 1-forms

$$\begin{aligned} \omega_1 &= dx + dy + dz \\ \omega_2 &= (y + z) dx + (z + x) dy + (x + y) dz \\ \omega_3 &= yz dx + zxy dy + xydz. \end{aligned} \quad (5)$$

Computing the resulting determinant, we see that the 1-forms  $\omega_i$ ,  $i = 1, 2, 3$ , are functionally dependent on the set  $S$ , defined by the equation  $(x - y)(y - z)(z - x) = 0$ , and functionally independent elsewhere (i.e. *regular points*). Consider now the vector fields which span locally, at regular points, the pairwise intersections of kernels of the above 1-forms, i.e.,

$$\begin{aligned} \ker \omega_2 \cap \ker \omega_3 &= \text{span}\{X_1\}, \\ \ker \omega_3 \cap \ker \omega_1 &= \text{span}\{X_2\}, \\ \ker \omega_1 \cap \ker \omega_2 &= \text{span}\{X_3\}. \end{aligned} \quad (6)$$

Our goal in what follows is to prove the stochastic connectivity property with respect to the almost-Riemannian structure induced on  $\mathbb{R}^2$  by the distribution  $\mathcal{D} = \text{span}\{X_1, X_2, X_3\}$ .

## References

- [1] A. A. Agrachev, U. Boscain, M. Sigalotti, *A Gauss-Bonnet-like formula on two-dimensional almost-Riemannian manifolds*, Discrete Contin. Dyn. Syst., 20,4 (2008), 801-822.
- [2] A. G. Ladde, G. S. Ladde, *An Introduction to Differential Equations II: Stochastic Modeling, Methods and Analysis*, World Scientific, Singapore, 2013.
- [3] A. Bellaïche, J. J. Risler (eds.), *Sub-Riemannian Geometry*, Progress in Mathematics 144, Birkhäuser, Basel, 1996.
- [4] O. Calin, D. C. Chang, *Sub-Riemannian Geometry: General Theory and Examples*, EMIA 126, Cambridge University Press, Cambridge, 2009.
- [5] O. Calin, C. Udriște, *Geometric Modeling in Probability and Statistics*, Springer, 2014.
- [6] O. Calin, C. Udriște, I. Țevy, *A stochastic variant of Chow-Rashevski Theorem on the Grushin distribution*, Balkan J. Geom. Appl., 19, 1 (2014), 1-12.
- [7] O. Calin, C. Udriște, I. Țevy, *Stochastic Sub-Riemannian geodesics on Grushin distribution*, Balkan J. Geom. Appl., 19, 2 (2014), 37-49.
- [8] C. H. Chang, D. C. Chang, B. Gaveau, P. Greiner, H. P. Lee, *Geometric analysis on a step 2 Grushin operator*, Bull. Inst. Math. Acad. Sinica (New Series) 4, 2 (2009), 119-188.
- [9] D. C. Chang, Y. Li, *SubRiemannian geodesics in the Grushin plane*, J. Geom. Anal. 22 (2012), 800-826.
- [10] W. L. Chow, *Über Systeme von linearen partiellen Differentialgleichungen erster Ordnung*, Math. Ann. 177 (1939), 98-105.
- [11] L. Hörmander, *Hypoelliptic second order differential operators*, Acta. Math. 119 (1967), 147-171.
- [12] R. Montgomery, *A Tour of Subriemannian Geometries, Their Geodesics and Applications*, Math Surveys and Monographs 91, AMS, Providence, RI, 2002.
- [13] B. Øksendal, *Stochastic Differential Equations*, 6-th ed., Springer, 2003.
- [14] P. K. Rashevskii, *About connecting two points of complete nonholonomic space by admissible curve*, Uch. Zapiski Ped. Institut. K. Liebknechta, 2 (1938), 83-94.
- [15] T. Țurcanu, C. Udriște, *Stochastic perturbation and connectivity based on Grushin distribution*, U.P.B. Sci. Bull., Series A, to appear.
- [16] T. Țurcanu, C. Udriște, *Stochastic perturbation and connectivity based on Grushin distribution*, U. Politeh. Bucharest Sci. Bull. Ser. A Appl. Math. Phys., 79, 1 (2017), 3-10.
- [17] T. Țurcanu, *On subRiemannian geodesics associated to a Grushin operator*, Appl. Anal., ID: 1268685.
- [18] T. Țurcanu, C. Udriște, *Stochastic accessibility on Grushin-type manifolds*, Statist. Probab. Lett., 125 (2017), 196-201.

## **Stability analysis of some equilibrium points in a complex model for cells evolution in leukemia**

BORDEI Ana-Maria, BADRALEXI Irina, HALANAY Andrei

The analysis regarding the stability of some equilibrium points in a complex model considers the competition between the populations of healthy and leukemic cells, the asymmetric division and the immune system in response to the disease. Delay differential equations are used to describe the dynamics of healthy and leukemic cells in case of CML (Chronic Myeloid Leukemia). The system consists of 9 delay differential equations, the first equations from 1 to 4 describe the hematopoietic healthy and leukemic cells evolution, equations 5 – 9 describe the evolution of the immune cell populations involved in the immune response against CML. The system has four possible types of equilibrium points, denoted  $E_1$ ,  $E_2$ ,  $E_3$  and  $E_4$ . The study is focused on the situations  $E_3$ , when leukemia cells have entirely replaced the healthy ones and  $E_4$ , representing a chronic phase of the disease.